

1  
2  
3  
4  
5 1 **ACA-20-2164-Rev.Highlighted**  
6  
7

8  
9 2 **Exploring the potential of combining**  
10  
11  
12  
13 3 **chemometric approaches to model non-linear**  
14  
15  
16  
17 4 **multi-way data with quantitative purposes – A**  
18  
19  
20  
21  
22 5 **case study**  
23  
24  
25  
26  
27 6  
28  
29

30 7 Mónica Palomino Vasco<sup>1</sup>, Nielene M. Mora Díaz<sup>1</sup>, María I. Rodríguez-Cáceres<sup>1</sup>, María I. Acedo-  
31 8 Valenzuela<sup>1</sup>, Mirta R. Alcaraz<sup>2,3,\*</sup> and Héctor C. Goicoechea<sup>2,3</sup>  
32  
33 9

34  
35  
36  
37 10 <sup>1</sup>*Department of Analytical Chemistry and Research Institute on Water, Climate Change and*  
38 11 *Sustainability (IACYS), University of Extremadura, Badajoz, 06006, Spain*  
39 12

40 13 <sup>2</sup>*Laboratorio de Desarrollo Analítico y Quimiometría (LADAQ), Cátedra de Química Analítica*  
41 14 *I, Facultad de Bioquímica y Ciencias Biológicas, Universidad Nacional del Litoral, Ciudad*  
42 15 *Universitaria, Santa Fe (S3000ZAA), Argentina*  
43 16

44 17 <sup>3</sup>*Consejo Nacional de Investigaciones Científicas y Técnicas (CONICET), Godoy Cruz 2290*  
45 18 *CABA (C1425FQB), Argentina.*  
46 19  
47  
48  
49

50 20  
51  
52 21 

---

Corresponding author:

53 22 \*E-mail: malcaraz@fbc.unl.edu.ar (M.R. Alcaraz). Tel.: +54 342 4575206 x190  
54 23  
55  
56  
57  
58  
59  
60  
61  
62  
63  
64  
65

1  
2  
3  
4  
5  
6  
7  
8  
9  
10  
11  
12  
13  
14  
15  
16  
17  
18  
19  
20  
21  
22  
23  
24  
25  
26  
27  
28  
29  
30  
31  
32  
33  
34  
35  
36  
37  
38  
39  
40  
41  
42  
43  
44  
45  
46  
47  
48  
49  
50  
51  
52  
53  
54  
55  
56  
57  
58  
59  
60  
61  
62  
63  
64  
65

24 **Abstract**

25 Second-order based calibration methods have been widely investigated capitalizing on the  
26 inherent benefits of the data structure and the decomposition models, demonstrating that second-  
27 order advantage is a property that conspires to a high likelihood success in the resolution of  
28 systems of varying complexity. This work aims to demonstrate the applicability of a combined  
29 chemometric strategy to solve non-linear multivariate calibration systems in the presence of non-  
30 multilinear multi-way data. The determination of histamine by differential pulse voltammetry at  
31 different pH is presented as case study. The experimental system has the outstanding difficulty  
32 arisen from the large displacement along the potential axis by the pH, which was successfully  
33 overcome by implementation of the presented combined strategy. For data modeling, MCR-ALS,  
34 U-PLS/RBL and U-PCA/RBL-RBF were used. MCR-ALS allowed unraveling the non-linear  
35 behavior between the signal and the concentration, and extracting the underlying profiles of the  
36 constituent. Quantitative analysis was performed through the three models, and a comparative  
37 evaluation of the predictive performance was done. The best results were achieved with U-  
38 PCA/RBL-RBF (mean recovery= 101%) whereas, MCR-ALS yield the lowest mean recovery for  
39 all samples (70%)

42 *Keywords:* non-trilinear type 3 data; pH-voltammetry; non-linear regression model; MCR-ALS;  
43 U-PLS/RBL; ANNs

44

1  
2  
3  
4  
5  
6  
7  
8  
9  
10  
11  
12  
13  
14  
15  
16  
17  
18  
19  
20  
21  
22  
23  
24  
25  
26  
27  
28  
29  
30  
31  
32  
33  
34  
35  
36  
37  
38  
39  
40  
41  
42  
43  
44  
45  
46  
47  
48  
49  
50  
51  
52  
53  
54  
55  
56  
57  
58  
59  
60  
61  
62  
63  
64  
65

## 45 **1. Introduction**

46 Multivariate calibration techniques have been attracting the attention of researchers in  
47 several investigation fields. The interest in the use of multivariate analysis relies on the fact that  
48 the inclusion of multiple signals can significantly improve the applicability of quantitative  
49 analyses [1, 2].

50 The central purpose of multivariate calibration is to establish empirical models relating  
51 unselective multiple instrumental signals to known analyte concentrations, which are then  
52 utilized to predict the analyte concentration of the test sample [3]. The multivariate calibration  
53 methodologies are categorized into first-, second- or higher-order calibration in association to the  
54 instrumental modes of the acquired signal [4, 5]. One particularity of first-order calibration  
55 methods is the requirement of a large number of calibration samples that must contain similar  
56 composition than the target sample, i.e., to contain the same potential interferents, for the success  
57 of the resolution and the prediction [3]. Nonetheless, second- and higher-order calibration  
58 models outweigh this attribute through a property that enables to selectively identify the  
59 components of a mixture even in the presence of non-modeled constituents, which is universally  
60 known as “second-order advantage” [5, 6].

61 The evolution of the modern analytical instrumentation has facilitated the acquisition of  
62 multidimensional signals allowing to enlarge the chemical information that can be obtained from  
63 the system under study. Some of the most common analytical instruments can yield first-order  
64 data for a single sample (e.g., infrared spectrum [7], UV spectrum [8], DSC signals [9]), which  
65 are acquired as a unidimensional vector data array. Second-order data could be obtained with a  
unique instrument, but it can be generated by instrumental hyphenation or experimental setups,  
allowing arranging the signals in bidimensional data arrays, i.e., data matrix. For instance,

1  
2  
3  
4 68 excitation-emission fluorescence matrices [10], chromatography coupled to spectral detection  
5  
6 69 [11] and kinetic with spectral monitoring [12] are cases of second-order data acquisition.  
7  
8

9 70 In the literature, it is possible to find several techniques for multivariate quantitative  
10  
11 71 analysis. Notwithstanding this great diversity of methods offers exceptional versatility in the  
12  
13 72 development of quantitative models, it usually leaves the analyst uncertain as to which is the  
14  
15 73 most appropriate for a given set of data. This situation is not a trivial matter since each data set  
16  
17 74 comprises particular underlying factors, e.g., noise level, signal overlapping, among others, that  
18  
19 75 cannot be generalized. One of the underlying factors of the data that must be considered before  
20  
21 76 modeling is the data linearity. In this regard, it becomes necessary to make a distinction between  
22  
23 77 the types of linearity that can be observed in the multivariate calibration field.  
24  
25  
26  
27

28 78 First, it should be evaluated if the instrumental modes in which the data was collected are  
29  
30 79 mutually independent. This condition guarantees the concept of *multi-linearity* of the multiway  
31  
32 80 data. When lack of multi-linearity is observed, it is relevant to identify its origin to evaluate the  
33  
34 81 different strategies that can be implemented for the resolution. The lack of multi-linearity has  
35  
36 82 been well described elsewhere by Olivieri and Escandar, who introduced a classification for the  
37  
38 83 different types of non-linearity in three- and four-way data structures [4]. On the other hand, in  
39  
40 84 analytical chemistry, many quantitative procedures apply linear calibration models to describe  
41  
42 85 the relationship between the instrumental measurement (dependent variable) and the property of  
43  
44 86 interest (independent variable) [13]. However, there are systems in which the linear law is not  
45  
46 87 obeyed, e.g., violation of the Beer-Lambert law, and non-linear functions ought to be applied to  
47  
48 88 fit the data. Hence, the evaluation of the lack of linearity and multi-linearity is an unavoidable  
49  
50 89 start in any multivariate quantitative procedure.  
51  
52  
53  
54  
55  
56  
57  
58  
59  
60  
61  
62  
63  
64  
65

1  
2  
3  
4  
5  
6  
7  
8  
9  
10  
11  
12  
13  
14  
15  
16  
17  
18  
19  
20  
21  
22  
23  
24  
25  
26  
27  
28  
29  
30  
31  
32  
33  
34  
35  
36  
37  
38  
39  
40  
41  
42  
43  
44  
45  
46  
47  
48  
49  
50  
51  
52  
53  
54  
55  
56  
57  
58  
59  
60  
61  
62  
63  
64  
65

90           Among calibration models, partial least square (PLS), principal component analysis  
91 (PCA) or classical least square (CLS) are the most common algorithms [13] for first-order  
92 calibration methods, while unfolded-PLS and multi-way-PLS (U-PLS and N-PLS) are two of the  
93 used algorithms in second-order calibration procedures [14]. All these algorithms perform linear  
94 calibration models, i.e., linear regression modeling, and only data that conform to the principle of  
95 multi-linearity can be subjected to decomposition [13, 15]. Besides, parallel factor analysis  
96 (PARAFAC) [16] and multivariate curve resolution coupled to alternating least-squares (MCR-  
97 ALS) [17] are algorithms based on alternating least-square optimization that allows decomposing  
98 higher-order data and gathering *loadings*, which comprise the individual profiles of the  
99 constituents, and *scores*, that are the contribution of the analytes in each sample [18]. The  
100 obtained scores can be then utilized to build the proper regression model in predictive studies,  
101 even in systems where the analytical signals do not vary linearly with the analyte concentration.  
102 However, when the non-linear relationship between the dependent and the independent variable  
103 is present, artificial neural networks (ANNs) are the most common methods used in building the  
104 empirical non-linear calibration model [19]. ANNs are non-parametric techniques, so they do not  
105 assume any specific model form providing them with especial flexibility and ability to model  
106 diverse kind of data [20].

107           This work aims to demonstrate the applicability of a combined chemometric strategy to  
108 solve non-linear multivariate calibration systems in the presence of lack of multi-linearity in  
109 multi-way data. In this research, the quantitation of histamine in the presence of histidine by  
110 differential pulse voltammetry at different pH is presented as case study. These data represent an  
111 outstanding chemometrics challenge because of the large potential-displacements of the  
112 electroanalytical signal arisen from the pH variation. Moreover, for the best of our knowledge,

1  
2  
3  
4 113 no reports regarding second-order DPV-pH data coupled to chemometrics with quantitative aims  
5  
6 114 have been published yet.

7  
8  
9 115

## 10 11 116 **2. Experimental section**

### 12 13 14 117 *2.1. Chemical, reagents and samples*

15  
16 118 Histamine (HIM) and histidine (HIS) were purchased from Sigma-Aldrich (Stenheim,  
17  
18 Germany) and Fluka (Buchs, Switzerland), respectively. Boric acid (p.a.  $\text{H}_3\text{BO}_3$ ) was obtained  
19 119 from Merck (Darmstadt, Germany). Glacial acetic acid (HAc), *o*-phosphoric acid ( $\text{H}_3\text{PO}_4$ ),  
20  
21 120 sodium hydroxide (NaOH) and dimethylformamide (DMF), all of analytical grade, were  
22  
23 121 acquired from Panreac (Barcelona, Spain). Ultra-pure water was obtained with a Milli-Q  
24  
25 122 purification system from Millipore (Bedford, USA).  
26  
27  
28  
29 123

30  
31 124 Analytes stock solutions of  $500 \text{ mg L}^{-1}$  were prepared by dissolution of the appropriate  
32  
33 125 amount of the powder presentation in ultrapure water and stored under refrigeration in the dark.  
34  
35  
36 126 Britton-Robinson Buffer (BRB) was prepared by mixing the proper amount of  $\text{H}_3\text{BO}_3$ , HAc and  
37  
38 127  $\text{H}_3\text{PO}_4$ , in order to obtain a final concentration of  $40 \text{ mmol L}^{-1}$  of each substance. To perform the  
39  
40  
41 128 pH-dependent experiments, the pH of the BRB was adjusted with NaOH, as appropriate, prior to  
42  
43 129 the sample preparation.  
44  
45

46 130

### 47 48 131 *2.2. Calibration and validation samples*

49  
50 132 A calibration set of HIM pure standard sample was daily prepared in triplicate by  
51  
52  
53 133 transferring the proper aliquot of the analyte stock solutions and 2.0 mL of BRB of the  
54  
55 134 corresponding pH to a 10.00 mL volumetric flask and completing to the mark with ultra-pure  
56  
57  
58 135 water. The final HIM concentrations were ranging between 0.0 and  $10.0 \text{ mg mL}^{-1}$ .  
59  
60  
61  
62  
63  
64  
65

1  
2  
3  
4  
5  
6  
7  
8  
9  
10  
11  
12  
13  
14  
15  
16  
17  
18  
19  
20  
21  
22  
23  
24  
25  
26  
27  
28  
29  
30  
31  
32  
33  
34  
35  
36  
37  
38  
39  
40  
41  
42  
43  
44  
45  
46  
47  
48  
49  
50  
51  
52  
53  
54  
55  
56  
57  
58  
59  
60  
61  
62  
63  
64  
65

136 A sample validation set was built considering HIM concentrations different than those used  
137 for the calibration samples. In these samples, HIS was incorporated as non-modeled interferent  
138 in 3 different concentrations as detailed in Table 1. The validation samples were prepared as  
139 previously described for the calibration samples.

### 141 2.3. Instrumentation and experimental procedure

142 Differential pulse voltammetry (DPV) measurements were conducted using a Metrohm  
143 663 VA and an AUTOLAB PGSTAT 10 potentiostat/galvanostat (ECOChemie. Utrecht, The  
144 Netherlands) with General-Purpose Electrochemical software (GPES) version 4.9.006  
145 (ECOChemie. Utrecht, The Netherlands) for the data acquisition and instrument control.

146 The DPV experiments were carried out in a 10 mL cell using a conventional three-  
147 electrode system configuration including a 3.0 mm diameter glassy carbon electrode (GCE) as  
148 working electrode, an Ag/AgCl (saturated KCl) reference electrode and a 0.3 mm platinum wire  
149 auxiliary electrode, all of them commercially acquired (ECOChemie. Utrecht, The Netherlands).

150 At the beginning of the working day, the surface of the GCE was mechanically cleaned  
151 using a cotton pad soaked in DMF for 2 minutes and in ultrapure water for 30 seconds. Then, an  
152 electrochemical cleaning was made by applying three reduction cycles in the range of +1.5 –  
153 +0.9 V, at 15 mV s<sup>-1</sup>, with an amplitude of 0.05 V, to the supporting electrolyte solution. The  
154 supporting electrolyte solution consisted in a BRB solution adjusted at the appropriate  
155 experimental pH. After electrode conditioning, DPV measurements were conducted by scanning  
156 the potential range of +0.9 V to +1.5 V at a scanning rate of 15 mV s<sup>-1</sup>, with an amplitude of  
157 0.05 V. Between measurements, the surface of the electrode was regenerated through mechanical  
158 cleaning. All experiments were carried out at room temperature.

1  
2  
3  
4 159 For the pH measurements, a Crison Micro pH 501m (Barcelona, Spain) equipped with a  
5  
6  
7 160 combined glass/saturated calomel electrode, was used.  
8

#### 9 161 10 11 162 *2.4. Software* 12 13

14 163 Data processing and analysis were performed in MATLAB 2015b [21]. MCR-ALS GUI  
15  
16 164 2.0 [22] codes for MATLAB were freely downloaded from [www.mcr-als.info](http://www.mcr-als.info). U-PLS/RBL and  
17  
18  
19 165 U-PCA-RBL-RBF were implemented in MVC2 [23] and MVC1 [24], respectively, for which the  
20  
21 166 MATLAB codes are available at <http://www.iquir-conicet.gov.ar/eng/div5.php?area=12>. *i-*  
22  
23  
24 167 coshift [25-27] tool for MATLAB was acquired from <http://www.models.life.ku.dk/icoshift>.  
25

26 168 For baseline correction, a moving average procedure (peak width of 0.01), which is  
27  
28  
29 169 available in the GEPS software, was implemented (Figure S1).  
30

### 31 170 32 33 171 **3. Results and discussion** 34

#### 35 36 172 *3.1. General considerations* 37

##### 38 173 *3.1.1. Chemometrics in electroanalytical chemistry* 39

40  
41 174 Curiously, the number of publications reporting the use of chemometrics in  
42  
43 175 electrochemistry is small in comparison with the application of other analytical methodologies,  
44  
45  
46 176 such as spectroscopy or chromatography. This observation has been recently stated by Esteban *et*  
47  
48 177 *al.* in Ref [28] whose proposed the hypothesis that the dearth of research in this topic might be  
49  
50  
51 178 caused by the close relationship between mathematics and electrochemistry and, also, the lack of  
52  
53 179 linearity between the signal and the concentration of the electroactive species [29, 30].  
54  
55 180 Nevertheless, there is an ongoing interest in exploit the potentialities of electrochemical  
56  
57  
58  
59  
60  
61  
62  
63  
64  
65



1  
2  
3  
4 181 instrumentation by applying chemometrics and promote its use to solve electroanalytical  
5  
6 182 problems.

7  
8  
9 183 First-order calibration methods have been extensively used in electroanalytical chemistry  
10  
11 184 by the implementation of the classical calibration models as multi-linear regression (MLR), PLS  
12  
13  
14 185 or PCR, among others [30]. Moreover, higher-order calibration methods have been recently  
15  
16 186 explored and presented in several publications reporting the application of MCR-ALS, PLS-  
17  
18  
19 187 based methods and ANNs techniques for the predictive analysis of compounds in samples of  
20  
21 188 variate nature [31, [32](#)]. Among the electroanalytical techniques, differential pulse voltammetry  
22  
23  
24 189 (DPV) and stripping voltammetry (SP) are the most used for the acquisition of second-order data  
25  
26 190 with quantitative aims [29, 31, 33, 34]. However, some features inherent to the electrochemical  
27  
28  
29 191 systems are cumbersome and made difficult the direct implementation of a chemometric model.  
30  
31 192 One of the most common issues present in electrochemistry is the signal displacement by  
32  
33 193 empirical phenomena that leads to a lack of linearity of the signal-analyte concentration  
34  
35  
36 194 relationship and a loss of multi-linearity in the multi-way data. Hence, recent works are focused  
37  
38 195 on the development of new strategies that enable either the modeling of non-linear data [34] or  
39  
40  
41 196 the correction of shifted data [29, [35](#), [36](#)]. Nevertheless, there is a noticeable dearth of research in  
42  
43 197 this field when large signal-shifts occur, for example, as it is the case of the displacement along  
44  
45  
46 198 the potential axis of some irreversible signals as a function of the pH [29].

47  
48 199

## 50 200 *3.2. Data properties*

### 53 201 *3.2.1. Multi-linearity*

54  
55 202 When second-order data are obtained for a set of samples, the data matrices can be  
56  
57  
58 203 organized into a three-way structure, which can whether conform to the *low-rank trilinearity*



1  
2  
3  
4  
5  
6  
7  
8  
9  
10  
11  
12  
13  
14  
15  
16  
17  
18  
19  
20  
21  
22  
23  
24  
25  
26  
27  
28  
29  
30  
31  
32  
33  
34  
35  
36  
37  
38  
39  
40  
41  
42  
43  
44  
45  
46  
47  
48  
49  
50  
51  
52  
53  
54  
55  
56  
57  
58  
59  
60  
61  
62  
63  
64  
65

227           These observations lead to the conclusion that the multi-way data set, i.e., DPV-pH-  
228 concentration, is a severe case of non-trilinear type 3 data, since neither bilinearity in the DPV-  
229 pH nor bilinearity in the DPV-concentration arrays are fulfilled. It is worth to highlight that this  
230 is the first time that this type of non-trilinear data is used with quantitative purposes.

231           Under this complex scenario, several alternatives were implemented to carry out the  
232 chemometric modeling. After an in-depth evaluation of the possible strategies, the following  
233 procedure was achieved. Aiming to recover de bilinearity in the DPV-concentration data array, a  
234 shift correction procedure based in correlation shifting method (*i-coshift*) [25-27] was  
235 implemented since no shape distortions were observable. Figure 2 shows the DPV signals  
236 acquired at three different pH level for several concentrations before and after shifting  
237 correction.

\*\*\*\* Figure 2 \*\*\*\*

241           In this way, a bilinear DPV-concentration array at each pH was obtained. Nonetheless,  
242 the DPV peak shifts arisen from the pH change were not corrected since the large displacements  
243 between signals would hinder the right implementation of a correction strategy and, more  
244 importantly, would suppress the selectivity of the second-mode. This phenomenon is a  
245 troublesome situation for which solutions were comprehensively analyzed and are described in  
246 this work.

### 3.2.2. Regression model

1  
2  
3  
4  
5  
6  
7  
8  
9  
10  
11  
12  
13  
14  
15  
16  
17  
18  
19  
20  
21  
22  
23  
24  
25  
26  
27  
28  
29  
30  
31  
32  
33  
34  
35  
36  
37  
38  
39  
40  
41  
42  
43  
44  
45  
46  
47  
48  
49  
50  
51  
52  
53  
54  
55  
56  
57  
58  
59  
60  
61  
62  
63  
64  
65

249 To implement the most appropriate regression model, a first evaluation of the trend line  
250 describing the relationship between the dependent (DPV signal) and the independent variable  
251 (concentration of the analyte) at every pH was performed. Figure 3 shows the aligned DPV  
252 signals for the calibration set (1.0-10.0 mg L<sup>-1</sup>) acquired at pH 4, 6 and 9.

\*\*\*\* Figure 3 \*\*\*\*

253  
254  
255 A clear difference in the regression trend at the different pH levels is noticeable with the  
256 naked eye. However, to accurately establish a function that explains the regression model for the  
257 entire system, it is necessary to perform a thorough evaluation by decomposing the data through  
258 specific chemometric techniques. Hence, experimental data were subjected to MCR-ALS to  
259 explore the empirical behavior of the constituents.

### 3.3. Data modeling

#### 3.3.1. MCR-ALS

263 MCR-ALS is a wide-spread soft-modelling method that performs bilinear decomposition  
264 of a data matrix into two sets of profiles, which comprise relevant physicochemical information  
265 about the constituents of the system under study [17]. The application of this method has been  
266 successfully demonstrated in numerous situations proving its potential to reach significant  
267 results. It has been implemented for many purposes, either quantitative analysis [11, 40-42] or  
268 descriptive studies allowing unraveling the behavior of chemical or biological processes where  
269 species are totally or partly unknown [43-45]. In this matter, the fact that MCR-ALS can extract  
270 the individual contribution of the constituents when no prior information of the system is  
271 available is rather appealing, especially, for investigations of highly complex systems.

1  
2  
3  
4  
5  
6  
7  
8  
9  
10  
11  
12  
13  
14  
15  
16  
17  
18  
19  
20  
21  
22  
23  
24  
25  
26  
27  
28  
29  
30  
31  
32  
33  
34  
35  
36  
37  
38  
39  
40  
41  
42  
43  
44  
45  
46  
47  
48  
49  
50  
51  
52  
53  
54  
55  
56  
57  
58  
59  
60  
61  
62  
63  
64  
65

272 The bilinear decomposition of MCR-ALS is performed under the application of  
273 constraints that are implemented during the iterative ALS phase. It is well-documented that if no  
274 constraints are implemented, uncountable possible solutions that equivalently represent the  
275 system might be obtained. The most common constraints are non-negativity, unimodality and  
276 correspondence between species, which relies on chemical principles [46]. However, it has been  
277 proved that the application of a full set of constraints helps to diminish the range of feasible  
278 solutions, albeit not completely. This phenomenon is known as *rotational ambiguity* [47, 48].

279 With the spread of multivariate data analysis escorted by the evolution of analytical  
280 instrumentation, diverse data structures have arisen, that coerced chemometricians to explore  
281 new alternatives for the data modeling. Along those lines, MCR-ALS has evolved into a very  
282 versatile strategy for the modeling of a wide range of data structures. Even though MCR-ALS is  
283 a pure bilinear decomposition model, it has been extended to higher-order multivariate analysis,  
284 e.g., third-order data [49-51]. Moreover, it is well-known that first-order calibration models can  
285 perform a reliable prediction only in the case that test samples contain the same composition that  
286 the calibration samples; however, it has been demonstrated that this drawback can be overcome  
287 with the aid of MCR-ALS. Ahmadi et al. have proved the ability of soft-modelling methods in  
288 analyzing first-order data sets containing unmodeled components, in which the rotational  
289 ambiguity associated to the resolution is minimized by applying specific constraints during  
290 iteration [52]. In addition, Esteban's group has demonstrated that the implementation of  
291 constraints that model the signal feature shall enhance the performance of the MCR-ALS  
292 modeling [53-56].

293 In the present case, pH dimension is the bilinear breaking mode, whereas the  
294 concentration mode fulfils the concept of low-rank bilinearity. Thus, to perform a bilinear

1  
2  
3  
4 295 decomposition, the path of Ahmadi work was followed and a *first-order* MCR-ALS strategy was  
5  
6  
7 296 implemented by unfolding the DPV-pH data to arrays of lower dimension, i.e., an unfolded one-  
8  
9 297 way vector. To achieve the decomposition, a bilinear row-wise concatenated/column-wise  
10  
11  
12 298 augmented matrix was built. First, a DPV-pH vector was obtained by concatenating the aligned  
13  
14 299 DPV signals of the different pH for each evaluated sample. Then, the concatenated vector  
15  
16 300 corresponding to each calibration and validation samples were column-wise appended. Figure S2  
17  
18  
19 301 (supplementary material) graphically depicts the data arrangement used for MCR-ALS  
20  
21 302 decomposition.

22  
23  
24 303 To start the modeling, initial concentration estimates were obtained by a SIMPLISMA-  
25  
26 304 like procedure [57] and the number of components was evaluated through singular value  
27  
28  
29 305 decomposition (SVD). The imposed constraints during optimization were non-negativity of  
30  
31 306 concentration and spectral modes, correspondence among the species and normalization in  
32  
33 307 concentration. Voltammogram and concentration profiles achieved from the MCR-ALS  
34  
35  
36 308 decomposition for four validation samples containing  $4.0 \text{ mg mL}^{-1}$  of HIM and calibration data  
37  
38 309 set are shown in Fig. 4.

39  
40  
41 310  
42  
43 311 \*\*\*\*\* Figure 4 \*\*\*\*\*

44  
45 312  
46  
47  
48 313 As can be seen in Fig. 4, two components were necessary to describe the behavior of HIM  
49  
50 314 and one additional component was needed for the samples containing HIS as interferent. These  
51  
52  
53 315 results are in accordance with the afore-mentioned observations demonstrating that the  
54  
55 316 regression model follows both linear and non-linear behavior against concentration in  
56  
57  
58 317 dependence to the pH. By evaluation of the unfolded voltammogram profiles, it can be noticed

59  
60  
61  
62  
63  
64  
65

1  
2  
3  
4  
5  
6  
7  
8  
9  
10  
11  
12  
13  
14  
15  
16  
17  
18  
19  
20  
21  
22  
23  
24  
25  
26  
27  
28  
29  
30  
31  
32  
33  
34  
35  
36  
37  
38  
39  
40  
41  
42  
43  
44  
45  
46  
47  
48  
49  
50  
51  
52  
53  
54  
55  
56  
57  
58  
59  
60  
61  
62  
63  
64  
65

318 that the non-linear regression trend prevails at lower pHs, whereas linearity arises with rising the  
319 pH values. For the predictive analysis, a pseudo-univariate calibration model was built by using  
320 the scores obtained for the factor with linear trend. These scores were plotted against the nominal  
321 concentration of the analyte and a least-square regression model was implemented to fit the data.  
322 Scores against nominal concentrations are depicted in Fig. 5 and predictive results are  
323 summarized in Table 1.

\*\*\*\* Figure 5 \*\*\*\*

327 As can be appreciated, at a higher concentration of the interferent, the contribution of the  
328 analyte significantly diminishes (# *Sample 7, 8, 11 and 12* in Table 1). This effect is evidenced  
329 by performing a prediction analysis with the scores obtained for the factor with linear regression  
330 trend (the scores of the second factor were not considered in this study because of its unusual  
331 behavior against concentration). This effect can be the result of two different phenomena. One of  
332 them can be related to the possible interaction between the analyte and the interferent, in which  
333 the interferent precludes the analyte detection. Besides, it should be considered that in first-order  
334 MCR-ALS decomposition, rotational ambiguity is heavily present and gets relevant at higher  
335 concentration of the unmodeled component due to the strong signal overlapping [52].

336 Based on these observations, it can be concluded that linear multi-way calibration models  
337 cannot be applied and other methodologies that enable the prediction of the analyte in the  
338 presence of non-linear regression trend need to be explored.

339  
340 3.3.2. U-PLS/RBL

1  
2  
3  
4  
5  
6  
7  
8  
9  
10  
11  
12  
13  
14  
15  
16  
17  
18  
19  
20  
21  
22  
23  
24  
25  
26  
27  
28  
29  
30  
31  
32  
33  
34  
35  
36  
37  
38  
39  
40  
41  
42  
43  
44  
45  
46  
47  
48  
49  
50  
51  
52  
53  
54  
55  
56  
57  
58  
59  
60  
61  
62  
63  
64  
65

341 The unfolded multi-way extension of the renowned PLS method is the U-PLS  
342 methodology that performs decomposition to higher dimension arrays. U-PLS it is a multi-way  
343 extension of PLS methodology and operates after unfolding the multi-way data arrays into  
344 vectors [58]. Those algorithms are applicable on systems showing small deviations of trilinearity,  
345 although the second-order advantage is not achieved. The U-PLS methodology consists of  
346 performing the classical PLS model calibration with the unfolded calibration data (not including  
347 the test samples) using a suitable number of latent variables. If no potential interferents are  
348 expected in the test samples, the amplitude of residuals in the prediction step is in the order of  
349 the instrumental noise level. Then, the concentration ( $\hat{y}_i$ ) prediction of the sample is obtained  
350 through  $\hat{y}_i = \mathbf{t}_i^T \mathbf{v}$ , where  $\mathbf{t}_i$  is the score vector obtained for the sample data matrix and  $\mathbf{v}$  are the  
351 regression coefficients acquired from the U-PLS model. However, when interferents are present,  
352 the residuals are extraordinarily large in comparison to the instrumental noise and, consequently,  
353 this formulation is not suitable for the prediction of the samples. Hence, to overcome this  
354 situation, the test sample is subjected to the residual bilinearization (RBL) procedure that enables  
355 to separate the signal that is explained by calibration from the contribution of the potential  
356 interferents, which means, achieve the second-order advantage [58-60]. To put it succinctly, the  
357 residual variance of a test sample is estimated considering the matrix  $\mathbf{E}$  which comprise the  
358 residuals of the U-PLS model. In the RBL process, the  $\mathbf{E}$  matrix is subsequently subjected to  
359 SVD decomposition for which results contain information about the interferents. This  
360 information that is then added to rebuild the original data matrix. Last, during the residual  
361 minimization step, the loadings obtained in the calibration stage remains constant while the  
362 scores are adjusted to minimize the residual variance. At the end for the RBL process, when the  
363 scores of the test sample are adjusted, the concentration of the analyte can be properly estimated



1  
2  
3  
4  
5  
6  
7  
8  
9  
10  
11  
12  
13  
14  
15  
16  
17  
18  
19  
20  
21  
22  
23  
24  
25  
26  
27  
28  
29  
30  
31  
32  
33  
34  
35  
36  
37  
38  
39  
40  
41  
42  
43  
44  
45  
46  
47  
48  
49  
50  
51  
52  
53  
54  
55  
56  
57  
58  
59  
60  
61  
62  
63  
64  
65

364 [\[61, 62\]](#). The combination of U-PLS and RBL has already been described and demonstrated in  
365 the relevant literature [58, 60].

366 In the present case, as it is shown in Fig. 5, the regression model shows a noticeable  
367 global non-linear signal behavior. Hence, U-PLS/RBL was implemented because it is one of the  
368 most flexible linear second-order multivariate calibration techniques and can cope with mild  
369 non-linearities. The calibration step was carried out using the well-known leave-one-out  
370 methodology. It is worth noticing that for linear regression system, only one or two PLS factors  
371 are necessary to explain the model; however, in the present experimental system, four PLS  
372 factors were needed to model the complexity of the data. This fact supports the presence of non-  
373 linearity that was observed with the MCR-ALS analysis.

374 The best prediction results were obtained when two RBL components were included in  
375 the resolution, which explains the presence of the interferent in the test samples. Table 1  
376 comprises the prediction results obtained with the U-PLS/RBL model for the validation samples.  
377 These values are better - albeit rather low ( $\bar{R}\%$  82 %) - than those obtained from MCR-ALS. It is  
378 noticeable that the lower recoveries were obtained for those samples containing the highest  
379 amount of the unmodeled component, in accordance with the MCR-ALS results. This conclusion  
380 strength the fact that a possible interaction between analyte and interferent is present during  
381 detection.

### 383 3.3.3. Artificial neural networks

384 Artificial neural network (ANN) constitutes a family of multivariate nonparametric  
385 regression techniques, which, after a convenient training procedure, are able of learning the  
386 correlation of a set of predictor variables with the desired response. The ANN family can be

1  
2  
3  
4  
5  
6  
7  
8  
9  
10  
11  
12  
13  
14  
15  
16  
17  
18  
19  
20  
21  
22  
23  
24  
25  
26  
27  
28  
29  
30  
31  
32  
33  
34  
35  
36  
37  
38  
39  
40  
41  
42  
43  
44  
45  
46  
47  
48  
49  
50  
51  
52  
53  
54  
55  
56  
57  
58  
59  
60  
61  
62  
63  
64  
65

387 subdivided into three groups of techniques: 1) multi-layer perceptron networks (MLP), 2) radial  
388 basis functions (RBF), and 3) support vector machines (SVM) [62]. The first two are the most  
389 frequently reported in the literature to solve multivariate calibration problems.

Briefly, ANNs contain operating units called neurons, which are arrayed in three layers:  
391 1) input, 2) hidden, and 3) output layers. Input and output neurons correspond to the measured  
392 signals and the properties predicted by the model, respectively. The hidden nodes represent the  
393 computing core. During training or calibration process, each hidden and output node receives  
394 weighted contributions, that are then projected on a transfer function to generate a non-linear  
395 output. The procedure of learning consists of adjusting the relationship between signals and  
396 concentrations by modifying the weights related to the inter-neural connections. Thus, the final  
397 output is close to the nominal concentration value for the analyte [20].

In second-order data, the number of original variables comprised in the instrumental  
399 signal is usually large and contain redundant information. Then, the information can be  
400 compacted into a small number of latent variables. For instance, the principal components (PCs)  
401 or scores obtained by computing the explained variance of the unfolded training data can be used  
402 as the input layer. When unexpected components are in the test samples, its scores shall not be  
403 adequate for the analyte prediction using the trained ANN [63]. Hence, it is necessary to  
404 implement a strategy capable to indicate the sample as an outlier, to separate the contribution of  
405 the unexpected component from the analyte signal and, then, to build the calibration model to  
406 perform the analyte prediction. It has been reported that unfolded PC analysis coupled to RBL  
407 (U-PCA/RBL) and subsequent ANN modeling is an excellent alternative to cope with this  
408 situation [62, 63]. In this approach, the adjusted score vector  $t_u$  obtained at the end of the RBL  
409 process is introduced into the ANN network for the subsequent concentration prediction.

1  
2  
3  
4 410 In this work, the number of PCs used as input neurons was four, and two RBL factors  
5  
6 411 were necessary for the modeling with U-PCA-RBL and subsequent prediction. RBF was chosen  
7  
8  
9 412 to perform the calibration model and the implemented architecture was (4-10-1) for input-  
10  
11  
12 413 hidden-output layers, respectively. The prediction results are shown in Table 1. As can be  
13  
14 414 appreciated, the performance of U-PCA/RBL-RBF is superior in comparison to the linear  
15  
16 415 regression methods, yielding excellent recoveries values with a  $\bar{R}$ % of 101 % ( $s=8$ ).

18  
19 416 Figure 6.A depicts the relationship between the nominal and predicted concentration for  
20  
21 417 the three chemometric models and the corresponding least-square fitting lines. Figure 6.B shows  
22  
23  
24 418 the elliptical joint confidence region for the slope and the intercept of the linear regression  
25  
26 419 between the actual and predicted concentration, with a 95% confidence level, for each model.  
27  
28  
29 420 Moreover, Fig 6.A and 6.B indicate the theoretical point and line, respectively, for intercept=0  
30  
31 421 and slope=1 [64]. Noticing that the ellipse built for U-PCA/RBL-RBF contains the theoretical  
32  
33 422 expected value for the intercept and slope and, moreover, the fitting line of nominal vs predicted  
34  
35  
36 423 relationship overlaps the theoretical line. These results reinforce the fact that with an in-depth  
37  
38 424 evaluation of the system behavior leading the use of the proper chemometric tool is possible to  
39  
40  
41 425 leverage the predictive properties of an analytical methodology

42  
43 426  
44  
45 427 \*\*\*\*\* Figure 6 \*\*\*\*\*  
46  
47

48 428  
49  
50 429 \*\*\*\*\* Table 1 \*\*\*\*\*  
51  
52

53 430  
54  
55 431 **4. Conclusions**  
56  
57  
58  
59  
60  
61  
62  
63  
64  
65

1  
2  
3  
4  
5  
6  
7  
8  
9  
10  
11  
12  
13  
14  
15  
16  
17  
18  
19  
20  
21  
22  
23  
24  
25  
26  
27  
28  
29  
30  
31  
32  
33  
34  
35  
36  
37  
38  
39  
40  
41  
42  
43  
44  
45  
46  
47  
48  
49  
50  
51  
52  
53  
54  
55  
56  
57  
58  
59  
60  
61  
62  
63  
64  
65

432 Second-order based calibration methods have been widely investigated capitalizing on the  
433 inherent benefits of the data structure and the decomposition models, demonstrating that second-  
434 order advantage is a property that conspires to a high likelihood success in the resolution of  
435 systems of varying complexity.

436 In this work, a qualitative and quantitative analysis was performed by implementing  
437 parametric and non-parametric methodologies for the determination of histamine in the presence  
438 of histidine by differential pulse voltammetry at several pHs as case study.

439 First, MCR-ALS was performed to evaluate the empirical behavior of the constituents. It  
440 was proved that first-order data, built from unfolded second-order data, can be solved with the  
441 aid of MCR-ALS, allowing to separate the individual contribution of each sample constituent.  
442 Based on the acquired results, it was concluded that at least two regression models were  
443 necessary to perform the calibration of the analyte, one of which presents a pronounced non-  
444 linear behavior. Moreover, it was possible to unravel the presence of a potential interaction  
445 between the analyte and the interferent, phenomenon that was reinforced with the results  
446 achieved from U-PLS/RBL.

447 On the other hand, U-PCA/RBL combined with RBF modeling significantly outweigh the  
448 performance of the parametric models demonstrating the capability to handle non-multilinear  
449 data in non-linear regression systems.

450 The results allowed to demonstrate the importance of performing a comprehensive  
451 analysis to accurately select the method to implement for the resolution and thus obtain reliable  
452 results. The most remarkable accomplishment achieved in this work was the successful  
453 implementation of chemometric techniques to bear the foresee difficulty arisen from the large  
454 displacement along the potential axis by the pH, which, to the best of our knowledge and belief,

1  
2  
3  
4 455 has not been reported yet. The modeling of non-multilinear data has been a matter of paramount  
5  
6 456 interest for chemometricians and represents an outstanding challenge in the field of quantitative  
7  
8  
9 457 electroanalytical chemistry. The inception of this research line encourages the development of  
10  
11  
12 458 new chemometric methodologies that lead to a coercive expansion of its range of application.  
13

14 459

## 16 460 **Acknowledgements**

18  
19  
20 461 This work was supported by the Ministerio de Economía y Competitividad of Spain (Project  
21  
22 462 CTQ2017-82496-P) and the Junta of Extremadura (GR18041-research Group FQM003), both  
23  
24 463 co-financed by the European Funds for Regional Development. M.P.V. is grateful to the Junta de  
25  
26  
27 464 Extremadura for a FPI grant (PD16033). MRA and HCG are staff of CONICET and grateful to  
28  
29 465 CONICET (Consejo Nacional de Investigaciones Científicas y Técnicas, Project PIP 2015-0111)  
30  
31  
32 466 and ANPCyT (Agencia Nacional de Promoción Científica y Tecnológica, Project PICT 2017-  
33  
34 467 0340) for financial support.  
35  
36

37 468

39  
40 469

## 42 **References**

- 44  
45 [1] A.C. Olivieri, Recent advances in analytical calibration with multi-way data, *Anal. Methods*,  
46 4 (2012) 1876-1886.  
47 [2] A.C. Olivieri, Analytical Advantages of Multivariate Data Processing. One, Two, Three,  
48 Infinity?, *Anal. Chem.*, 80 (2008) 5713-5720.  
49 [3] A.C. Olivieri, *Introduction to Multivariate Calibration: A Practical Approach*, Springer  
50 International Publishing, Cham, 2018.  
51 [4] A.C. Olivieri, G.M. Escandar, *Practical Three-Way Calibration*, Elsevier, Waltham, USA,  
52 2014.  
53 [5] K.S. Booksh, B.R. Kowalski, Theory of Analytical Chemistry, *Anal. Chem.*, 66 (1994)  
54 782A-791A.  
55 [6] H.A.L. Kiers, A.K. Smilde, Some theoretical results on second-order calibration methods for  
56 data with and without rank overlap, *J. Chemom.*, 9 (1995) 179-195.  
57  
58  
59  
60  
61  
62  
63  
64  
65

- 1  
2  
3  
4 [7] C. Radulescu, R.L. Olteanu, C. Stih, M. Florescu, R.M. Stirbescu, S.G. Stanescu, C.M.  
5 Nicolescu, M. Bumbac, Chemometrics-based vibrational spectroscopy for Juglandis semen  
6 extracts investigation, *J. Chemom.*, 34 (2020) e3234.  
7  
8 [8] M. Albayrak, F. Demirkaya-Miloglu, O. Senol, E. Polatdemir, Design, optimization, and  
9 validation of chemometrics-assisted spectrophotometric methods for simultaneous determination  
10 of etodolac and thiocolchicoside in pharmaceuticals, *Journal of Analytical Science and*  
11 *Technology*, 10 (2019) 16.  
12  
13 [9] J. Tarrío-Saavedra, M. Francisco-Fernández, S. Naya, J. López-Beceiro, C. Gracia-  
14 Fernández, R. Artiaga, Wood identification using pressure DSC data, *J. Chemom.*, 27 (2013)  
15 475-487.  
16  
17 [10] W. Mbogning Feudjio, H. Ghalila, M. Nsangou, Y.G. Mbesse Kongbonga, Y. Majdi,  
18 Excitation-emission matrix fluorescence coupled to chemometrics for the exploration of essential  
19 oils, *Talanta*, 130 (2014) 148-154.  
20  
21 [11] M.R. Alcaraz, M.J. Culzoni, H.C. Goicoechea, Enhanced fluorescence sensitivity by  
22 coupling yttrium-analyte complexes and three-way fast high-performance liquid chromatography  
23 data modeling, *Anal. Chim. Acta*, 902 (2016) 50-58.  
24  
25 [12] M.R. Alcaraz, A. Schwaighofer, H. Goicoechea, B. Lendl, EC-QCL mid-IR transmission  
26 spectroscopy for monitoring dynamic changes of protein secondary structure in aqueous solution  
27 on the example of  $\beta$ -aggregation in alcohol-denatured  $\alpha$ -chymotrypsin, *Anal. Bioanal. Chem.*,  
28 408 (2016) 3933-3941.  
29  
30 [13] J.H. Kalivas, 3.01 - Calibration Methodologies, in: S.D. Brown, R. Tauler, B. Walczak,  
31 *Comprehensive Chemometrics*, Elsevier, Oxford, 2009, pp. 1-32.  
32  
33 [14] A.C. Olivieri, G.M. Escandar, H.C. Goicoechea, A.M. de la Peña, Chapter 7 - Unfolded and  
34 Multiway Partial Least-Squares with Residual Multilinearization: Fundamentals, in: A. Muñoz  
35 de la Peña, H.C. Goicoechea, G.M. Escandar, A.C. Olivieri, *Data Handling in Science and*  
36 *Technology*, Elsevier 2015, pp. 347-363.  
37  
38 [15] J. Ferré, 3.02 - Regression Diagnostics, in: S.D. Brown, R. Tauler, B. Walczak,  
39 *Comprehensive Chemometrics*, Elsevier, Oxford, 2009, pp. 33-89.  
40  
41 [16] R. Bro, PARAFAC. Tutorial and applications, *Chemom. Intell. Lab. Syst.*, 38 (1997) 149-  
42 171.  
43  
44 [17] A. de Juan, S.C. Rutan, R. Tauler, 2.19 - Two-Way Data Analysis: Multivariate Curve  
45 Resolution – Iterative Resolution Methods, in: S.D. Brown, R. Tauler, B. Walczak,  
46 *Comprehensive Chemometrics*, Elsevier, Oxford, 2009, pp. 325-344.  
47  
48 [18] K.S. Booksh, B. Bronk, J. Czege, 3.09 - Three-Way Calibration, in: S.D. Brown, R. Tauler,  
49 B. Walczak, *Comprehensive Chemometrics*, Elsevier, Oxford, 2009, pp. 379-412.  
50  
51 [19] F. Marini, 3.14 - Neural Networks, in: S.D. Brown, R. Tauler, B. Walczak, *Comprehensive*  
52 *Chemometrics*, Elsevier, Oxford, 2009, pp. 477-505.  
53  
54 [20] F. Despagne, D.L. Massart, Neural networks in multivariate calibration, *Analyst*, 123 (1998)  
55 157R-178R.  
56  
57 [21] Matlab, The MathWorks Inc., Natick, MA, USA, 2015.  
58  
59 [22] J. Jaumot, A. De Juan, R. Tauler, MCR-ALS GUI 2.0: New features and applications,  
60 *Chemom. Intell. Lab. Syst.*, 140 (2015) 1-12.  
61  
62 [23] A.C. Olivieri, H.-L. Wu, R.-Q. Yu, MVC2: A MATLAB graphical interface toolbox for  
63 second-order multivariate calibration, *Chemom. Intell. Lab. Syst.*, 96 (2009) 246-251.  
64  
65 [24] A.C. Olivieri, H.C. Goicoechea, F.A. Iñón, MVC1: an integrated MatLab toolbox for first-  
order multivariate calibration, *Chemom. Intell. Lab. Syst.*, 73 (2004) 189-197.

- 1  
2  
3  
4 [25] F. Savorani, G. Tomasi, S.B. Engelsen, Alignment of 1D NMR Data using the iCoshift  
5 Tool: A Tutorial, *Magnetic Resonance in Food Science: Food for Thought*, The Royal Society of  
6 Chemistry 2013, pp. 14-24.
- 7 [26] G. Tomasi, F. Savorani, S.B. Engelsen, icoshift: An effective tool for the alignment of  
8 chromatographic data, *J. Chromatogr. A*, 1218 (2011) 7832-7840.
- 9 [27] F. Savorani, G. Tomasi, S.B. Engelsen, icoshift: A versatile tool for the rapid alignment of  
10 1D NMR spectra, *J. Magn. Reson.*, 202 (2010) 190-202.
- 11 [28] M. Esteban, M.C. Ariño-Blasco, J.M. Díaz-Cruz, 4.01 - Chemometrics in  
12 Electrochemistry☆, in: S.D. Brown, R. Tauler, B. Walczak, *Comprehensive Chemometrics*  
13 (Second Edition), Elsevier, Oxford, 2020, pp. 1-31.
- 14 [29] A. Alberich, J.M. Díaz-Cruz, C. Ariño, M. Esteban, Potential shift correction in multivariate  
15 curve resolution of voltammetric data. General formulation and application to some experimental  
16 systems, *Analyst*, 133 (2008) 112-125.
- 17 [30] J.M. Díaz-Cruz, M. Esteban, C. Ariño, Multivariate Calibration, in: J.M. Díaz-Cruz, M.  
18 Esteban, C. Ariño, *Chemometrics in Electroanalysis*, Springer International Publishing, Cham,  
19 2019, pp. 87-129.
- 20 [31] A.R. Jalalvand, H.C. Goicoechea, D.N. Rutledge, Applications and challenges of multi-way  
21 calibration in electrochemical analysis, *TrAC, Trends Anal. Chem.*, 87 (2017) 32-48.
- 22 [32] I. Cukrowski, J. Havel, Evaluation of Equilibria with a Use of Artificial Neural Networks  
23 (ANN): I. Artificial Neural Networks and Experimental Design as a Tool in Electrochemical  
24 Data Evaluation for Fully Inert Metal Complexes, *Electroanalysis*, 12 (2000) 1481-1492.
- 25 [33] M. Kooshki, H. Abdollahi, S. Bozorgzadeh, B. Haghighi, Second-order data obtained from  
26 differential pulse voltammetry: Determination of tryptophan at a gold nanoparticles decorated  
27 multiwalled carbon nanotube modified glassy carbon electrode, *Electrochim. Acta*, 56 (2011)  
28 8618-8624.
- 29 [34] A.R. Jalalvand, M.-B. Gholivand, H.C. Goicoechea, T. Skov, Generation of non-multilinear  
30 three-way voltammetric arrays by an electrochemically oxidized glassy carbon electrode as an  
31 efficient electronic device to achieving second-order advantage: Challenges, and tailored  
32 applications, *Talanta*, 134 (2015) 607-618.
- 33 [35] A. Alberich, J.M. Díaz-Cruz, C. Ariño, M. Esteban, Combined use of the potential shift  
34 correction and the simultaneous treatment of spectroscopic and electrochemical data by  
35 multivariate curve resolution: analysis of a Pb(II)-phytochelatin system. *The Analyst*, 133 (2008)  
36 470-477.
- 37 [36] J.M. Díaz Cruz, J. Sanchís, E. Chekmeneva, C. Ariño, M. Esteban, Non-linear multivariate  
38 curve resolution analysis of voltammetric pH titrations. *Analyst*, 135 (2010) 1653-1662.
- 39 [37] A.V. Schenone, M.J. Culzoni, A.D. Campiglia, H.C. Goicoechea, Total synchronous  
40 fluorescence spectroscopic data modeled with first- and second-order algorithms for the  
41 determination of doxorubicin in human plasma, *Anal. Bioanal. Chem.*, 405 (2013) 8515-8523.
- 42 [38] A.V. Schenone, A. de Araújo Gomes, M.J. Culzoni, A.D. Campiglia, M.C.U. de Araújo,  
43 H.C. Goicoechea, Modeling nonbilinear total synchronous fluorescence data matrices with a  
44 novel adapted partial least squares method, *Anal. Chim. Acta*, 859 (2015) 20-28.
- 45 [39] P. Puthongkham, S.T. Lee, B.J. Venton, Mechanism of Histamine Oxidation and  
46 Electropolymerization at Carbon Electrodes, *Anal. Chem.*, 91 (2019) 8366-8373.
- 47 [40] M.R. Alcaraz, A.V. Schenone, M.J. Culzoni, H.C. Goicoechea, Modeling of second-order  
48 spectrophotometric data generated by a pH-gradient flow injection technique for the  
49 determination of doxorubicin in human plasma, *Microchem. J.*, 112 (2014) 25-33.
- 50  
51  
52  
53  
54  
55  
56  
57  
58  
59  
60  
61  
62  
63  
64  
65

- 1  
2  
3  
4 [41] M.R. Alcaraz, L. Vera Candiotti, M.J. Culzoni, H.C. Goicoechea, Ultrafast quantitation of  
5 six quinolones in water samples by second-order capillary electrophoresis data modeling with  
6 multivariate curve resolution–alternating least squares, *Anal. Bioanal. Chem.*, 406 (2014) 2571-  
7 2580.  
8  
9 [42] C.M. Teglia, S.M. Azcarate, M.R. Alcaráz, H.C. Goicoechea, M.J. Culzoni, Exploiting the  
10 synergistic effect of concurrent data signals: Low-level fusion of liquid chromatographic with  
11 dual detection data, *Talanta*, 186 (2018) 481-488.  
12 [43] M.R. Alcaraz, A. Aguirre, H.C. Goicoechea, M.J. Culzoni, S.E. Collins, Resolution of  
13 intermediate surface species by combining modulated infrared spectroscopy and chemometrics,  
14 *Anal. Chim. Acta*, 1049 (2019) 38-46.  
15 [44] A. Schwaighofer, M.R. Alcaraz, L. Lux, B. Lendl, pH titration of  $\beta$ -lactoglobulin monitored  
16 by laser-based Mid-IR transmission spectroscopy coupled to chemometric analysis, *Spectrochim.*  
17 *Acta A Mol. Biomol. Spectrosc.*, 226 (2020) 117636.  
18 [45] R. Brasca, A.-M. Kelterer, M. Maeder, M.R. Alcaraz, M.J. Culzoni, Quantum chemical  
19 computation-based strategy for alternating least squares initialization in multivariate curve  
20 resolution analysis of spectral-pH data, *Microchem. J.*, 140 (2018) 183-188.  
21 [46] R. Tauler, M. Maeder, A. de Juan, 2.24 - Multiset Data Analysis: Extended Multivariate  
22 Curve Resolution, in: S.D. Brown, R. Tauler, B. Walczak, *Comprehensive Chemometrics*,  
23 Elsevier, Oxford, 2009, pp. 473-505.  
24 [47] M.R. Alcaraz, M.J. Culzoni, G.A. Ibañez, V.A. Lozano, A.C. Olivieri, On second-order  
25 calibration based on multivariate curve resolution in the presence of highly overlapped profiles,  
26 *Anal. Chim. Acta*, 1096 (2020) 53-60.  
27 [48] A. Golshan, H. Abdollahi, S. Beyramysoltan, M. Maeder, K. Neymeyr, R. Rajkó, M.  
28 Sawall, R. Tauler, A review of recent methods for the determination of ranges of feasible  
29 solutions resulting from soft modelling analyses of multivariate data, *Anal. Chim. Acta*, 911  
30 (2016) 1-13.  
31 [49] M.R. Alcaraz, G.G. Siano, M.J. Culzoni, A. Muñoz de la Peña, H.C. Goicoechea, Modeling  
32 four and three-way fast high-performance liquid chromatography with fluorescence detection  
33 data for quantitation of fluoroquinolones in water samples, *Anal. Chim. Acta*, 809 (2014) 37-46.  
34 [50] M. Montemurro, G.G. Siano, M.R. Alcaraz, H.C. Goicoechea, Third order  
35 chromatographic-excitation–emission fluorescence data: Advances, challenges and prospects in  
36 analytical applications, *TrAC, Trends Anal. Chem.*, 93 (2017) 119-133.  
37 [51] A. Malik, R. Tauler, Extension and application of multivariate curve resolution-alternating  
38 least squares to four-way quadrilinear data–obtained in the investigation of pollution patterns on  
39 Yamuna River, India—A case study, *Anal. Chim. Acta*, 794 (2013) 20-28.  
40 [52] G. Ahmadi, R. Tauler, H. Abdollahi, Multivariate calibration of first-order data with the  
41 correlation constrained MCR-ALS method, *Chemom. Intell. Lab. Syst.*, 142 (2015) 143-150.  
42 [53] J. Mendieta, M.S. Díaz-Cruz, R. Tauler, M. Esteban, Application of Multivariate Curve  
43 Resolution to Voltammetric Data: II. Study of Metal-Binding Properties of the Peptides, *Anal.*  
44 *Biochem.*, 240 (1996) 134-141.  
45 [54] M.S. Díaz-Cruz, J. Mendieta, R. Tauler, M. Esteban, Multivariate Curve Resolution of  
46 Cyclic Voltammetric Data: Application to the Study of the Cadmium-Binding Properties of  
47 Glutathione, *Anal. Chem.*, 71 (1999) 4629-4636.  
48 [55] S. Cavanillas, J.M. Díaz-Cruz, C. Ariño, M. Esteban, Parametric signal fitting by gaussian  
49 peak adjustment: A new multivariate curve resolution method for non-bilinear voltammetric  
50 measurements, *Anal. Chim. Acta*, 689 (2011) 198-205.  
51  
52  
53  
54  
55  
56  
57  
58  
59  
60  
61  
62  
63  
64  
65



- 1  
2  
3  
4 [56] S. Cavanillas, N. Serrano, J.M. Díaz-Cruz, C. Ariño, M. Esteban, Parametric Signal Fitting  
5 by Gaussian Peak Adjustment: implementation of 2D transversal constraints and its application  
6 for the determination of pKa and complexation constants by differential pulse voltammetry,  
7 Analyst, 138 (2013) 2171-2180.  
8  
9 [57] W. Windig, J. Guilment, Interactive self-modeling mixture analysis, Anal. Chem., 63 (1991)  
10 1425-1432.  
11 [58] A.C. Olivieri, On a versatile second-order multivariate calibration method based on partial  
12 least-squares and residual bilinearization: Second-order advantage and precision properties, J.  
13 Chemom., 19 (2005) 253-265.  
14 [59] G.M. Escandar, H.C. Goicoechea, A. Muñoz de la Pena, A.C. Olivieri, Second- and higher-  
15 order data generation and calibration: a tutorial, Anal. Chim. Acta, 806 (2014) 8-26.  
16 [60] J. Öhman, P. Geladi, S. Wold, Residual bilinearization. Part 1: Theory and algorithms, J.  
17 Chemom., 4 (1990) 79-90.  
18 [61] A. de Araújo Gomes, M.R. Alcaraz, H.C. Goicoechea, M.C. Araújo, The Successive  
19 Projections Algorithm for interval selection in trilinear partial least-squares with residual  
20 bilinearization, Anal. Chim. Acta, 811 (2014) 13-22.  
21 [62] A. García-Reiriz, P.C. Damiani, M.J. Culzoni, H.C. Goicoechea, A.C. Olivieri, A versatile  
22 strategy for achieving the second-order advantage when applying different artificial neural  
23 networks to non-linear second-order data: Unfolded principal component analysis/residual  
24 bilinearization, Chemom. Intell. Lab. Syst., 92 (2008) 61-70.  
25 [63] A.C. Olivieri, A combined artificial neural network/residual bilinearization approach for  
26 obtaining the second-order advantage from three-way non-linear data, J. Chemom., 19 (2005)  
27 615-624.  
28 [64] J. Riu, F.X. Rius, Method comparison using regression with uncertainties in both axes,  
29 TrAC, Trends Anal. Chem., 16 (1997) 211-216.  
30  
31  
32  
33  
34  
35  
36  
37  
38  
39  
40  
41  
42  
43  
44  
45  
46  
47  
48  
49  
50  
51  
52  
53  
54  
55  
56  
57  
58  
59  
60  
61  
62  
63  
64  
65

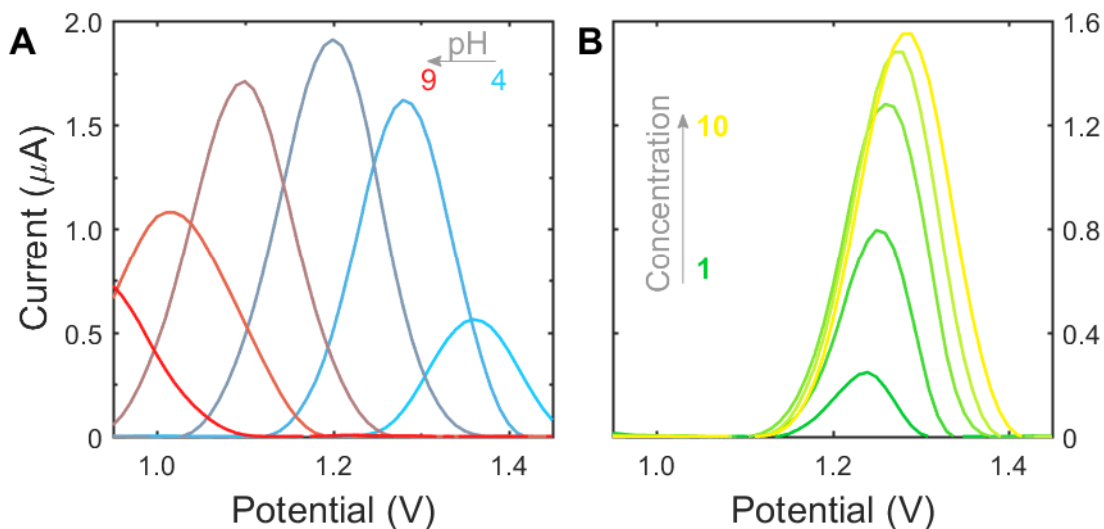


**Figure 1.** (A) Differential pulse voltammograms obtained at GEC in BRB solution containing of  $5.0 \text{ mg L}^{-1}$  HIM at the pH range of 4-9 (from cyan to red lines) and the (B) Differential pulse voltammograms obtained at GEC registered for concentrations of 1.0-10.0  $\text{mg L}^{-1}$  HIM at pH 6.

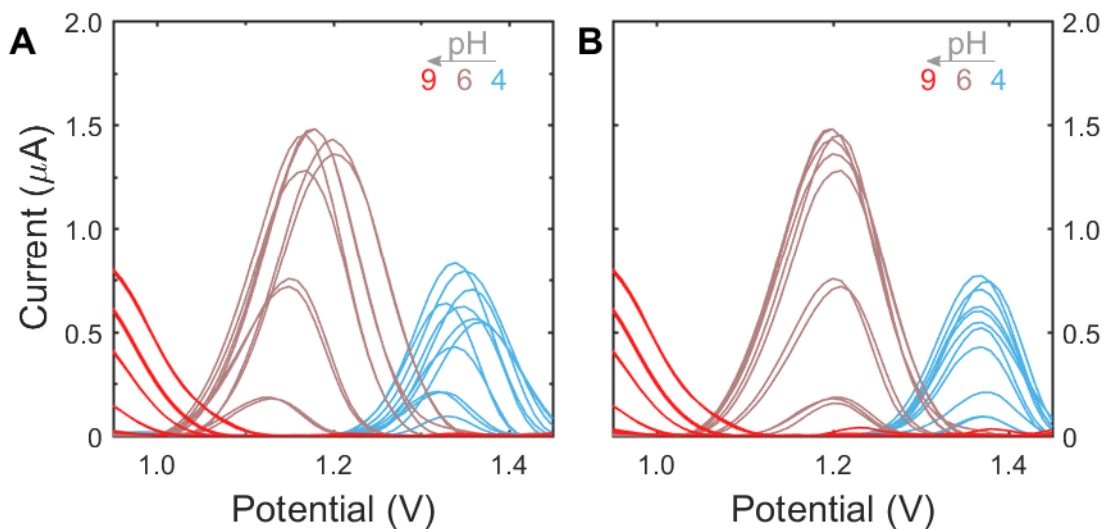


**Figure 2.** (A) Original and (B) aligned DPV signals acquired for several concentrations of HIM at pH 4 (cyan) 6 (purple) and 9 (red).

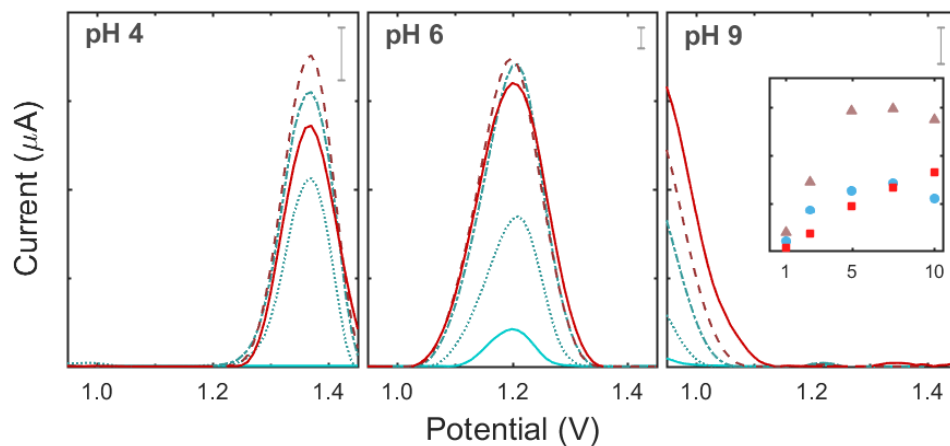


**Figure 3.** Aligned DPV signals of  $1.0 \text{ mg L}^{-1}$  (solid cyan line) and  $10.0 \text{ mg L}^{-1}$  (solid red line) of HIM at pH 4, 6 and 9. DPV signals of  $2.5 \text{ mg L}^{-1}$  (dotted line),  $5.0 \text{ mg L}^{-1}$  (dash-dotted line) and  $7.5 \text{ mg L}^{-1}$  (dashed line)  $\text{mg L}^{-1}$  of HIM are shown. Grey bars indicate the current of  $0.1 \text{ } \mu\text{A}$ . Inset: maximum current intensity against concentration at pH 4 (cyan) 6 (purple) and 9 (red).

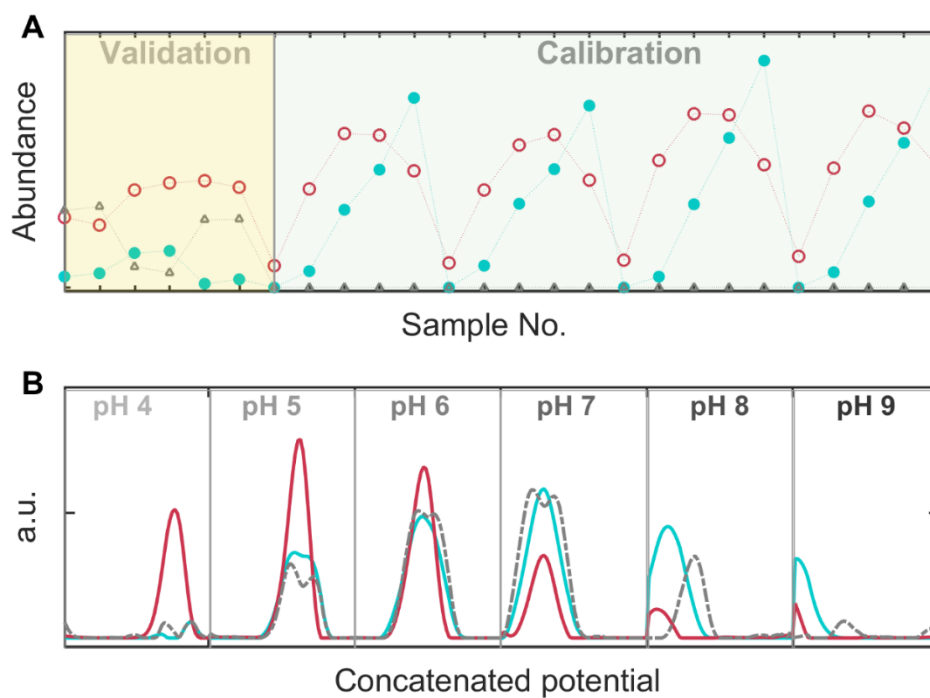


**Figure 4.** (A) Concentration and (B) unfolded voltammogram profiles acquired after MCR-ALS decomposition of DVP-pH signals. The first six samples correspond to validation samples containing  $4.0 \text{ mg L}^{-1}$  HIM (empty red and full cyan circles) and  $25.0$ ,  $5.0$  and  $15.0 \text{ mg L}^{-1}$  HIS (grey triangles) in duplicate, respectively.

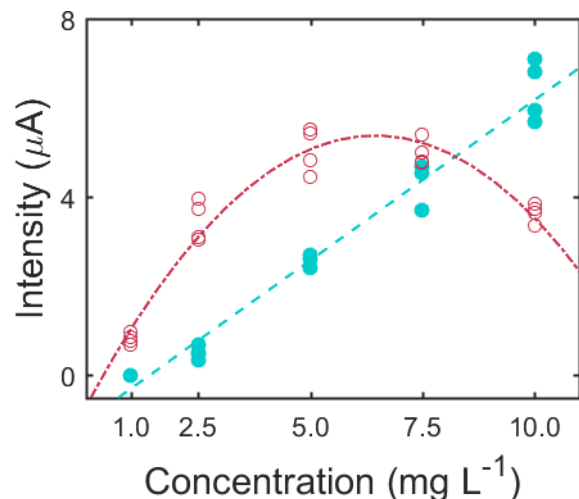


**Figure 5.** MCR-ALS concentration scores obtained from the calibration signals of HIM against nominal concentration. Scores of first (full cyan dots) and second (empty red dots) MCR-ALS factors show the linear and nonlinear regression trends, respectively. Dashed cyan line and dash-dotted red line are the fitted lines through linear and quadratic function, respectively.

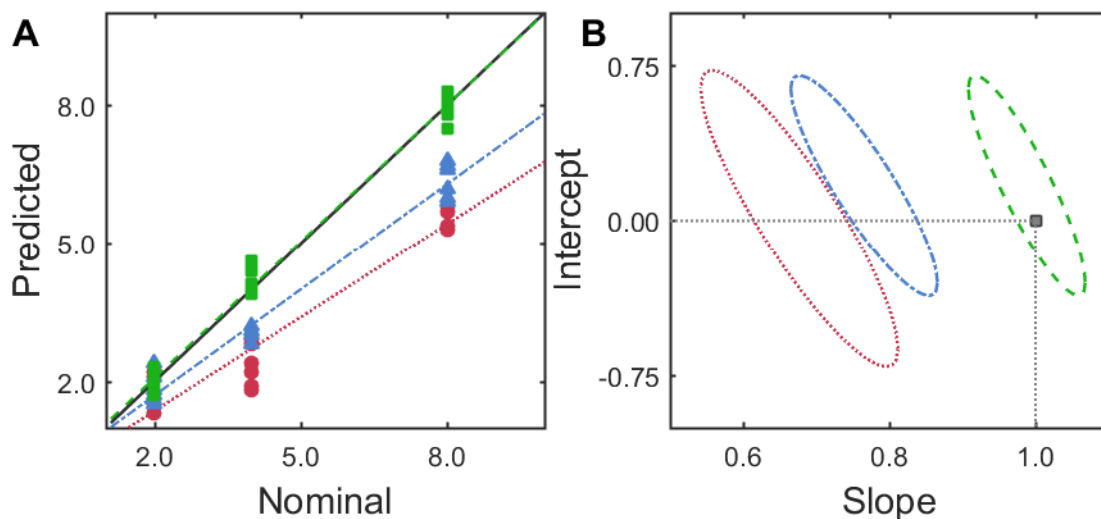


**Figure 6.** (A) Nominal against predicted concentrations of HIM (in  $\text{mg mL}^{-1}$ ) and the corresponding least-square fitting lines. (B) Elliptical joint of confidence region (95% confidence level) for the slope and the intercept of the linear regression between the nominal and the predicted concentrations of HIM. MCR-ALS (dotted red line), U-PLS/RBL (dash-dotted blue line) and U-PCA/RBL-RBF (dashed green line). Results for MCR-ALS are in red, U-PLS/RBL in blue and U-PCA/RBL-RBF are in green. The theoretical regression line (A) and the ideal point (B) (slope=1, intercept=0) are shown in black.

**Table 1.** Recovery results obtained from validation samples using parametric and nonparametric methodologies.

# Sample	HIM (mg L <sup>-1</sup> ) <sup>a</sup>			HIS <sup>b</sup> (mg L <sup>-1</sup> )	
	Nominal	Predicted			
		MCR/ALS	UPLS/RBL		U-PCA/RBL - RBF
<b>1</b>	2.0	2.1 (105)	2.4 (120)	2.2 (110)	25.0
<b>2</b>	2.0	2.2 (110)	2.1 (105)	1.8 (90)	25.0
<b>3</b>	2.0	1.3 (65)	1.7 (85)	1.9 (95)	5.0
<b>4</b>	2.0	1.5 (75)	1.8 (90)	2.1 (105)	5.0
<b>5</b>	2.0	1.3 (65)	1.6 (75)	2.3 (115)	15.0
<b>6</b>	2.0	1.3 (65)	1.5 (74)	1.7 (85)	15.0
<b>7</b>	4.0	2.2 (55)	3.0 (75)	4.4 (110)	25.0
<b>8</b>	4.0	2.4 (60)	3.1 (78)	4.6 (115)	25.0
<b>9</b>	4.0	2.9 (73)	3.2 (80)	3.9 (98)	5.0
<b>10</b>	4.0	2.8 (70)	3.1 (78)	3.9 (98)	5.0
<b>11</b>	4.0	1.8 (45)	2.8 (70)	4.1 (103)	15.0
<b>12</b>	4.0	1.9 (48)	2.8 (70)	4.1 (103)	15.0
<b>13</b>	8.0	5.7 (71)	5.9 (70)	7.5 (94)	25.0
<b>14</b>	8.0	5.8 (73)	6.0 (75)	8.1 (101)	25.0
<b>15</b>	8.0	5.3 (66)	6.2 (78)	7.9 (99)	5.0
<b>16</b>	8.0	5.4 (68)	6.8 (85)	8.3 (104)	5.0
<b>17</b>	8.0	5.4 (68)	6.7 (84)	7.8 (98)	15.0
<b>18</b>	8.0	5.7 (71)	6.6 (83)	8.2 (103)	15.0
$\bar{R}\%$ <sup>c</sup>		<b>70 (s=16)</b>	<b>82 (s=12)</b>	<b>101 (s=8)</b>	

<sup>a</sup> Recoveries (%) are between parenthesis

<sup>b</sup> HIS as an interferent

<sup>c</sup> Mean recovery in %

**Table 1.** Recovery results obtained from validation samples using parametric and nonparametric methodologies.

# Sample	HIM (mg L <sup>-1</sup> ) <sup>a</sup>				HIS <sup>b</sup> (mg L <sup>-1</sup> )
	Nominal	Predicted			
		MCR/ALS	UPLS/RBL	U-PCA/RBL - RBF	
<b>1</b>	2.0	2.1 (105)	2.4 (120)	2.2 (110)	25.0
<b>2</b>	2.0	2.2 (110)	2.1 (105)	1.8 (90)	25.0
<b>3</b>	2.0	1.3 (65)	1.7 (85)	1.9 (95)	5.0
<b>4</b>	2.0	1.5 (75)	1.8 (90)	2.1 (105)	5.0
<b>5</b>	2.0	1.3 (65)	1.6 (75)	2.3 (115)	15.0
<b>6</b>	2.0	1.3 (65)	1.5 (74)	1.7 (85)	15.0
<b>7</b>	4.0	2.2 (55)	3.0 (75)	4.4 (110)	25.0
<b>8</b>	4.0	2.4 (60)	3.1 (78)	4.6 (115)	25.0
<b>9</b>	4.0	2.9 (73)	3.2 (80)	3.9 (98)	5.0
<b>10</b>	4.0	2.8 (70)	3.1 (78)	3.9 (98)	5.0
<b>11</b>	4.0	1.8 (45)	2.8 (70)	4.1 (103)	15.0
<b>12</b>	4.0	1.9 (48)	2.8 (70)	4.1 (103)	15.0
<b>13</b>	8.0	5.7 (71)	5.9 (70)	7.5 (94)	25.0
<b>14</b>	8.0	5.8 (73)	6.0 (75)	8.1 (101)	25.0
<b>15</b>	8.0	5.3 (66)	6.2 (78)	7.9 (99)	5.0
<b>16</b>	8.0	5.4 (68)	6.8 (85)	8.3 (104)	5.0
<b>17</b>	8.0	5.4 (68)	6.7 (84)	7.8 (98)	15.0
<b>18</b>	8.0	5.7 (71)	6.6 (83)	8.2 (103)	15.0
$\bar{R}\%$ <sup>c</sup>		<b>70 (s=16)</b>	<b>82 (s=12)</b>	<b>101 (s=8)</b>	

<sup>a</sup> Recoveries (%) are between parenthesis

<sup>b</sup> HIS as an interferent

<sup>c</sup> Mean recovery in %

Figure 1  
[Click here to download high resolution image](#)

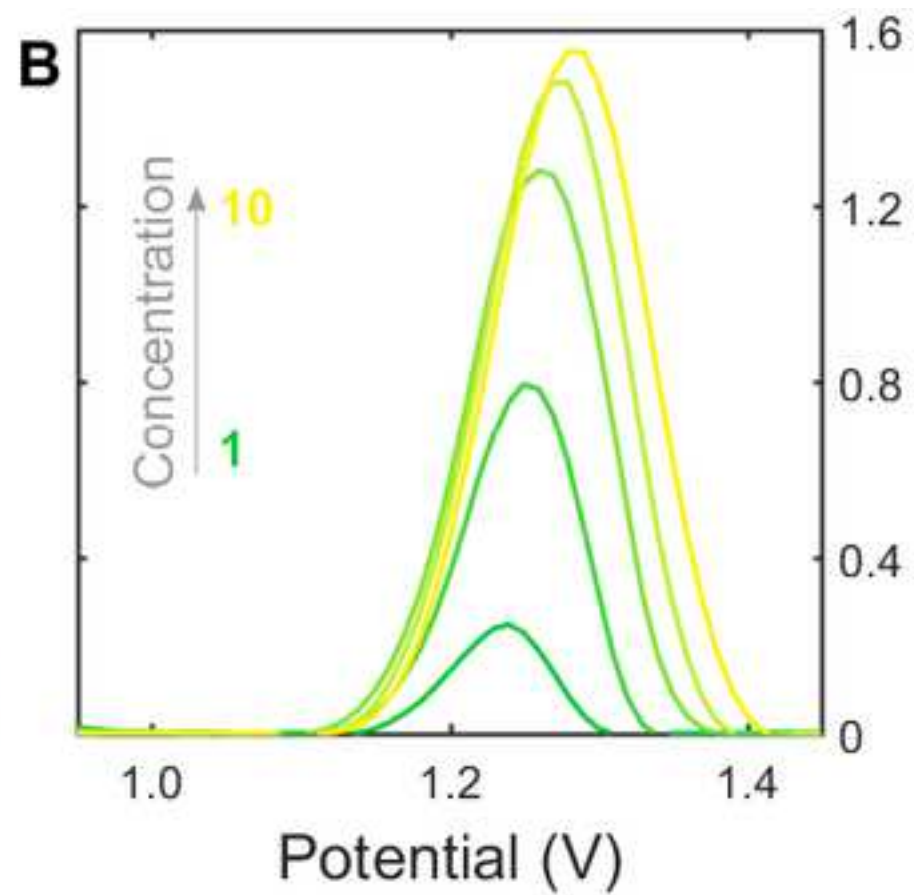
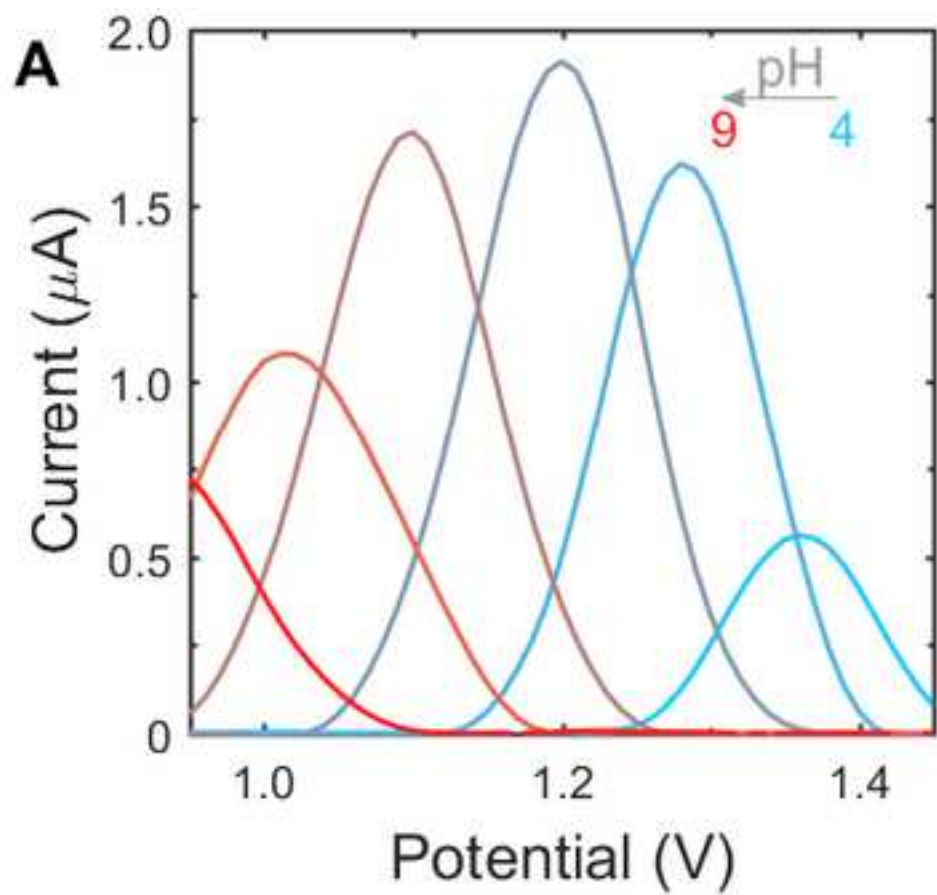


Figure 2

[Click here to download high resolution image](#)

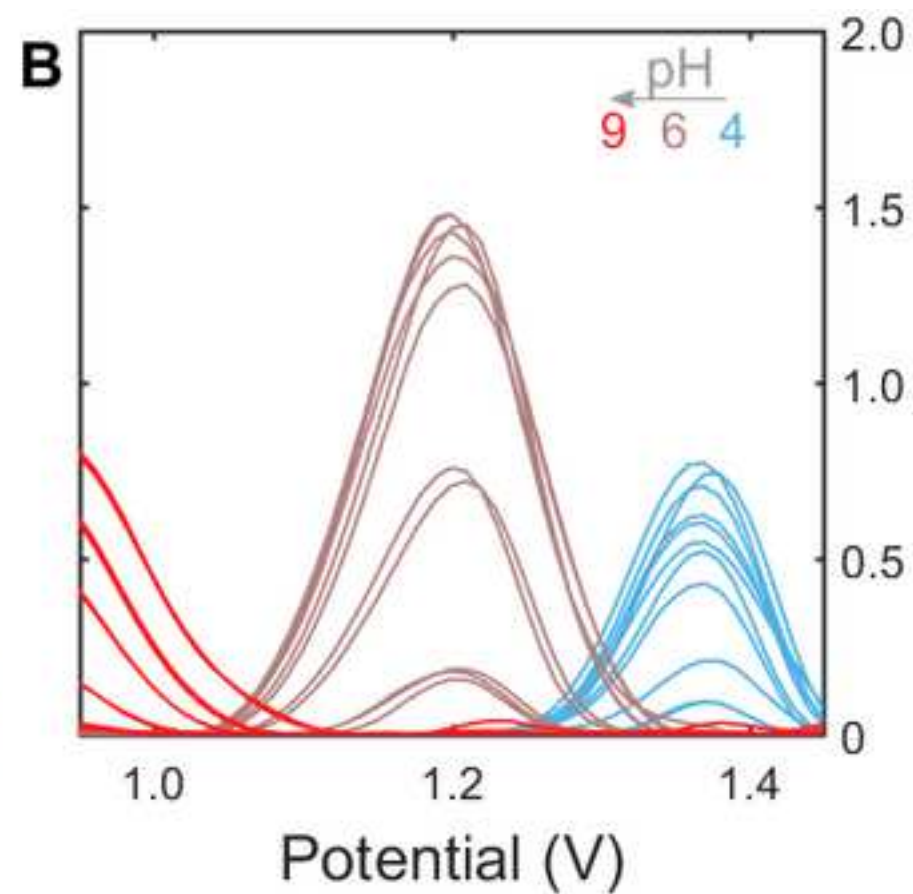
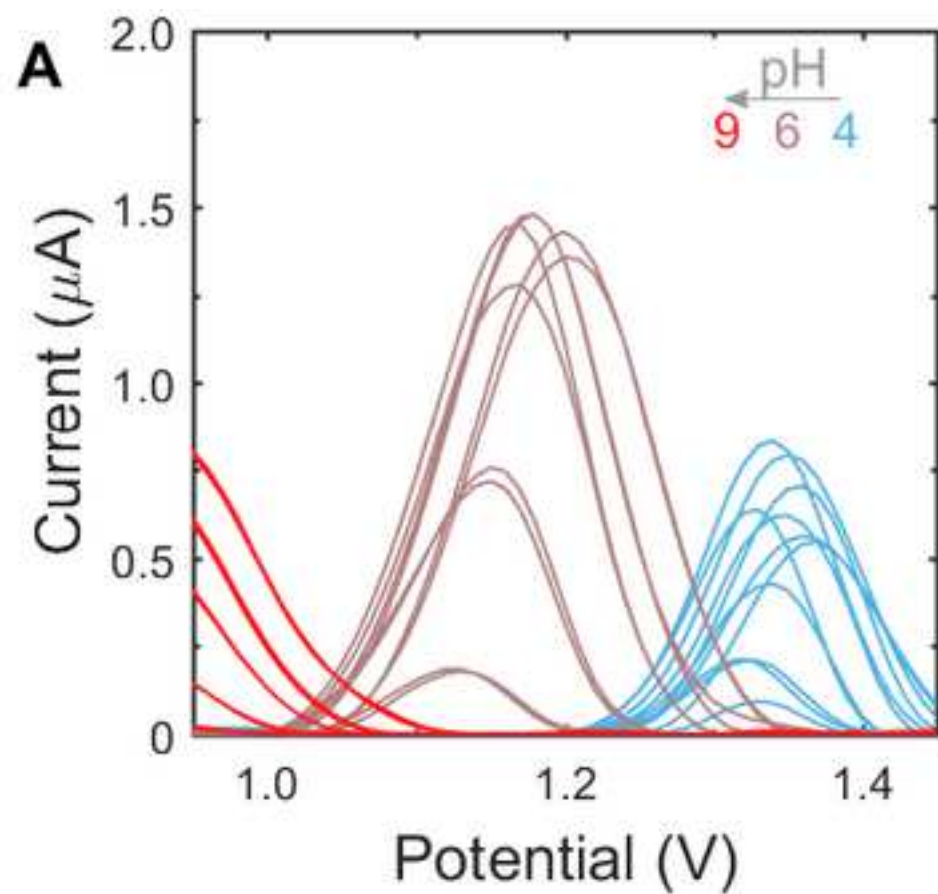




Figure 3  
[Click here to download high resolution image](#)

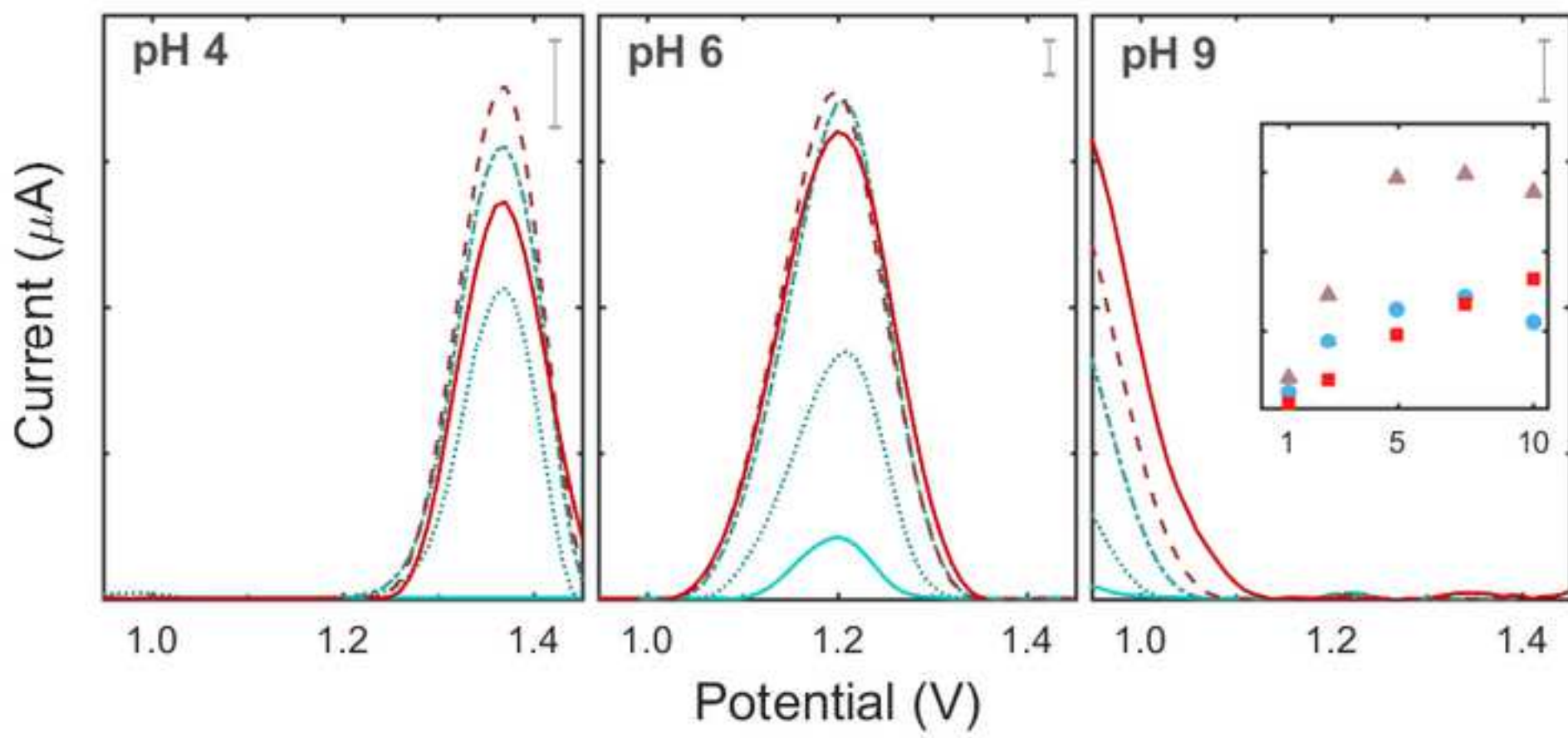


Figure 4  
[Click here to download high resolution image](#)

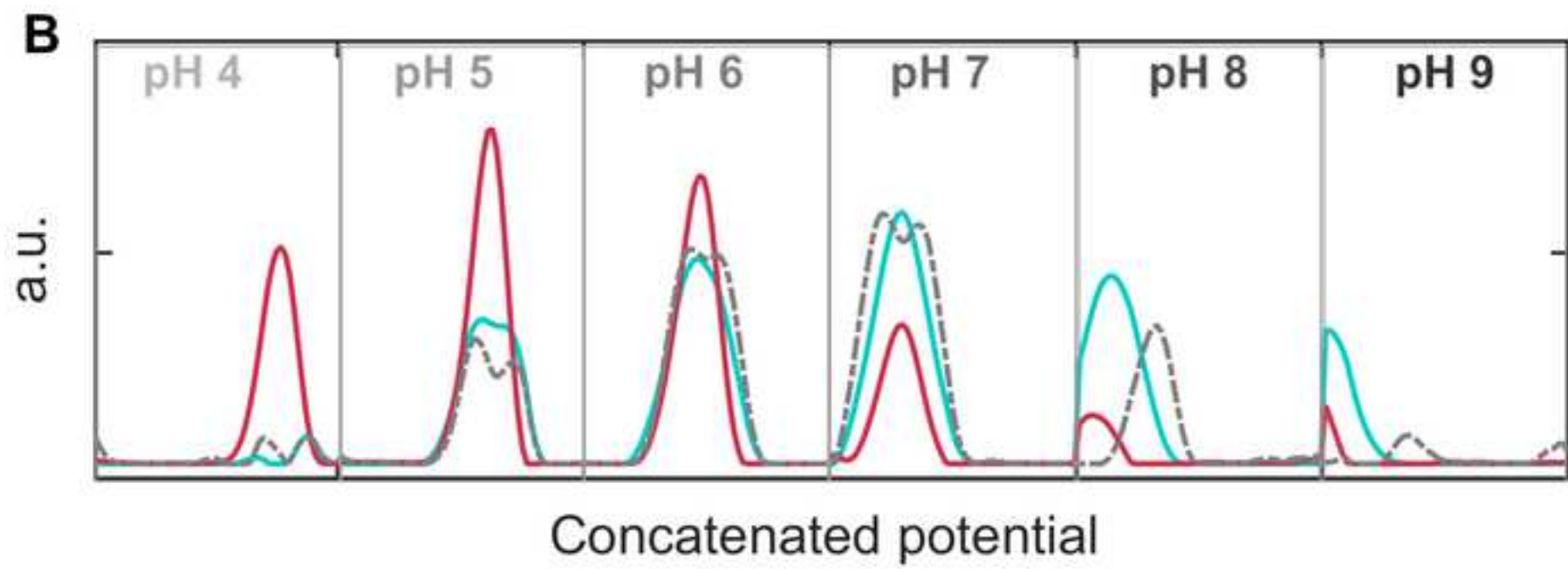
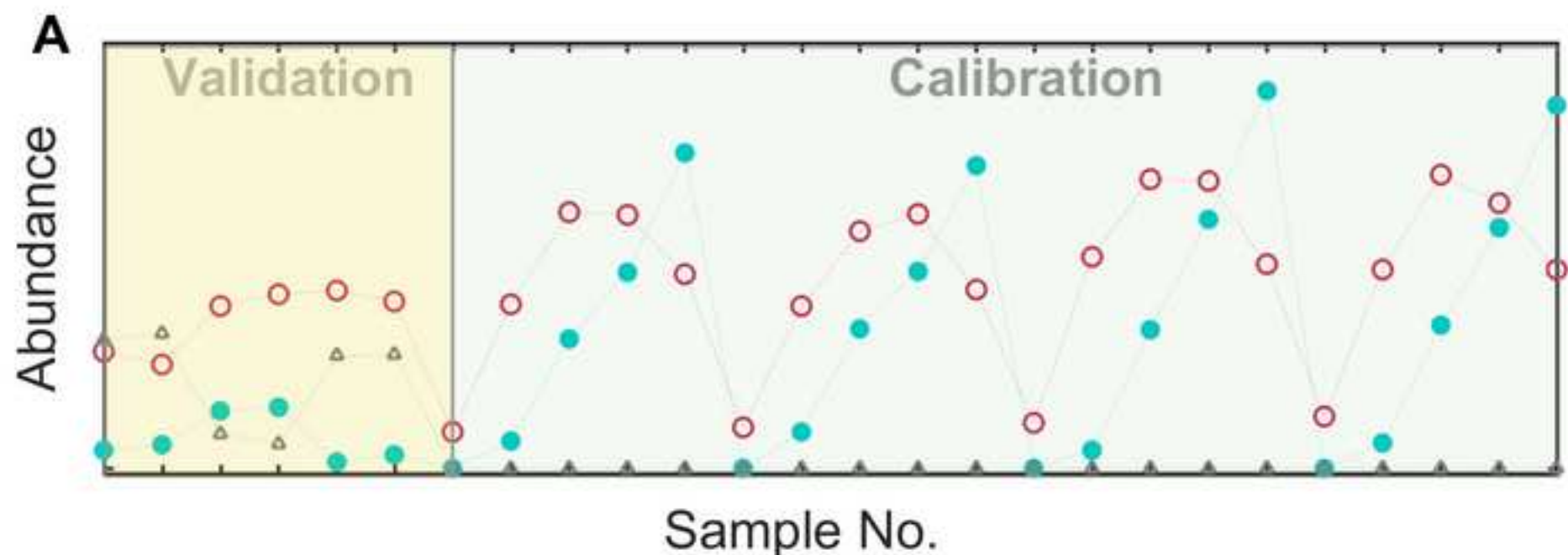


Figure 5  
[Click here to download high resolution image](#)

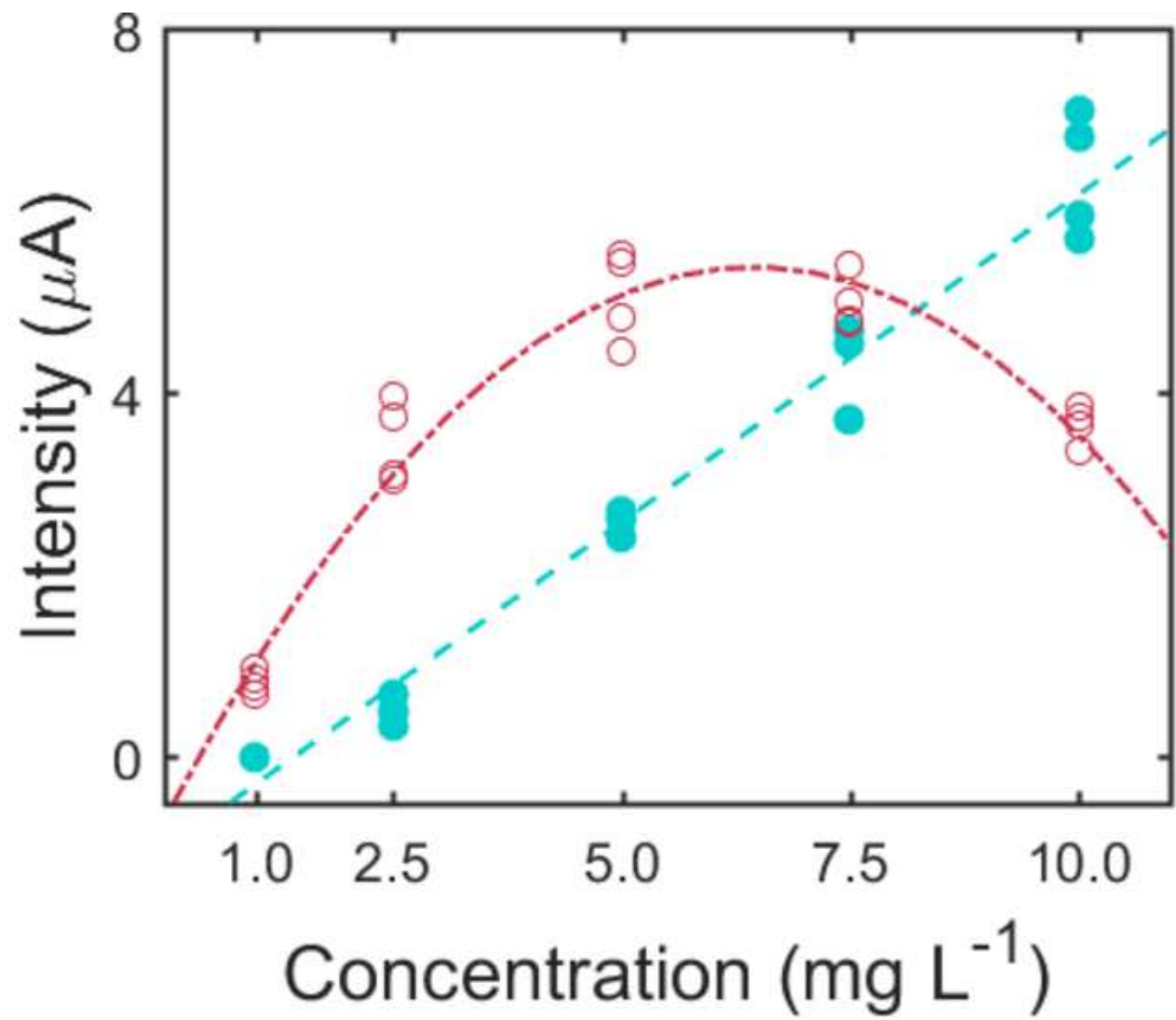
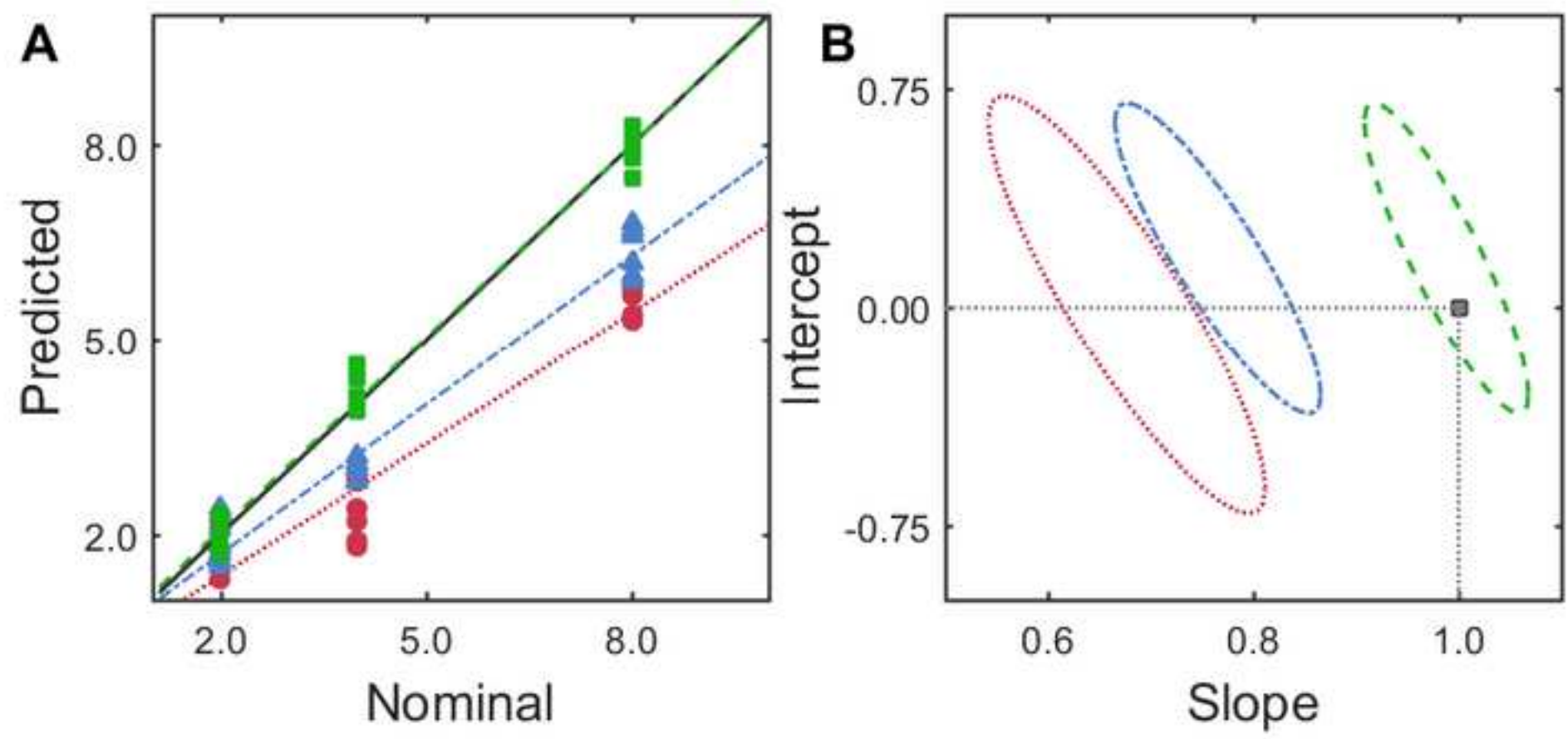


Figure 6  
[Click here to download high resolution image](#)



# Exploring the potential of combining chemometric approaches to model non-linear multi-way data – A case study

Mónica Palomino-Vasco<sup>1</sup>, Nielen Mora-Díez<sup>1</sup>, [María Isabel Rodríguez-Cáceres](#), [María](#)

[Isabel Acedo-Valenzuela](#), Mirta R. Alcaraz<sup>2,3\*</sup> and Héctor C. Goicoechea<sup>2,3</sup>

<sup>1</sup> *Department of Analytical Chemistry and Research Institute on Water, Climate Change and Sustainability (IACYS), University of Extremadura, Badajoz, 06006, Spain*

<sup>2</sup> *Laboratorio de Desarrollo Analítico y Quimiometría (LADAQ), Cátedra de Química Analítica I, Facultad de Bioquímica y Ciencias Biológicas, Universidad Nacional del Litoral, Ciudad Universitaria, Santa Fe (S3000ZAA), Argentina*

<sup>3</sup> *Consejo Nacional de Investigaciones Científicas y Técnicas (CONICET), Godoy Cruz 2290 CABA (C1425FQB), Argentina.*

---

Corresponding author:

\*E-mail: [malcaraz@fcb.unl.edu.ar](mailto:malcaraz@fcb.unl.edu.ar) (M.R. Alcaraz). Tel.: +54 342 4575206 x190

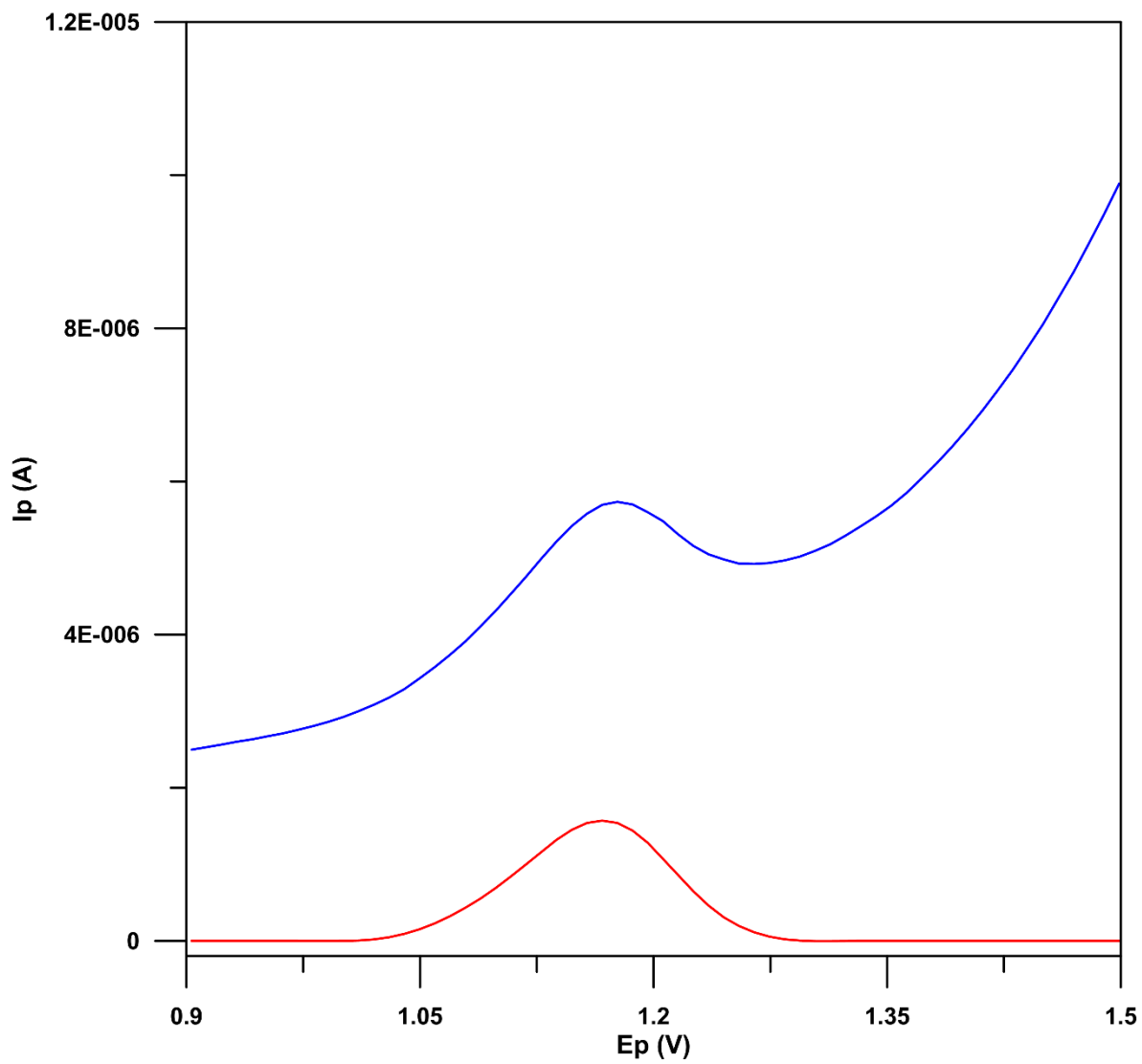


Figure S-1. Example of the baseline correction employing GPES. Voltammogram without any treatment in blue, and after baseline correction in red.

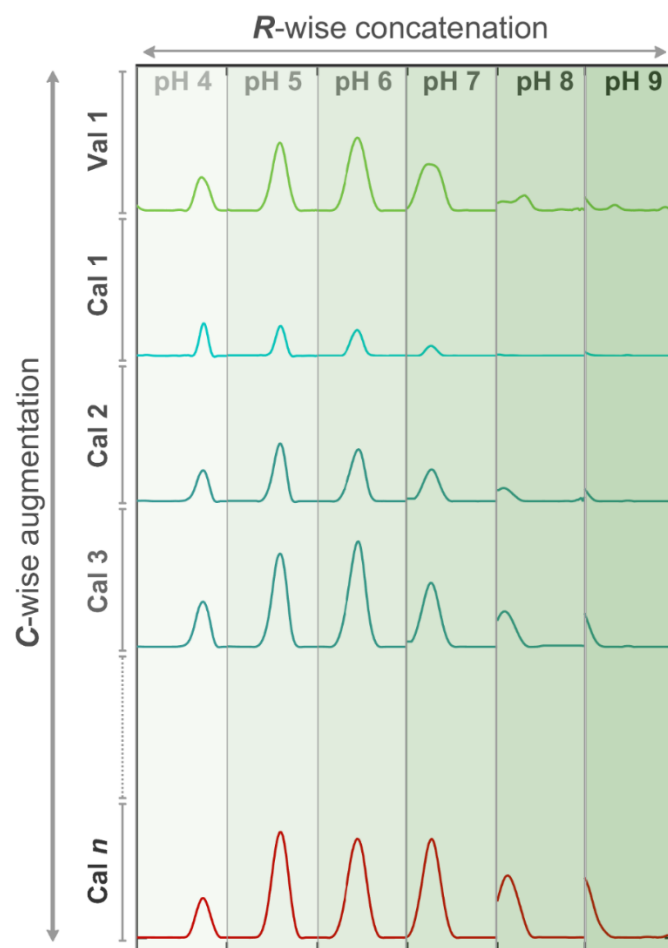


Figure S-2. Data arrangement for MCR-ALS resolution. Cal 1- $n$  are de DPV-pH signals corresponding to the calibration samples and Val 1 is the corresponding signal of validation samples. (SUPPLEMENTARIA?)